Reflections in a Pool of Mercury: An Experimental and Theoretical Study of the Interaction Between Electromagnetic Radiation and a Liquid Metal

AARON N. BLOCH* AND STUART A. RICE
Department of Chemistry and The James Franck Institute, The University of Chicago, Chicago, Illinois 60637
(Received 2 December 1968)

The conclusion of Schulz and of Wilson and Rice that the low-energy absolute reflectance of liquid mercury obeys the simple Drude formula is confirmed by new measurements made at near-normal incidence in the wavelength range 0.5–30 μ. The difficulties inherent in obtaining such data are discussed, and a precise and sensitive double-beam infrared reflectance spectrometer, constructed for the purpose of overcoming these difficulties, is described. The results described must be reconciled with recent ellipsometric studies, carried out independently at several different laboratories, in which the apparent optical constants of liquid mercury were found to be substantially higher than those predicted by the Drude theory. From an examination of the solutions of Maxwell's equations describing the interaction of electromagnetic radiation with an inhomogeneous conductor, it is shown that such anomalous optical behavior is to be expected for a liquid metal whose surface is not a geometric boundary, but a transition zone over which the properties of the system vary from those of the bulk metal to those of the contact medium. To test the plausibility of this model, a simple form for the conductivity profile across this transition zone is assumed, and the surface parameters characteristic of that profile are varied to fit the observed ellipsometric and reflectometric data. Excellent agreement between theory and experiment is found for a variety of choices of the parameters, provided that the conductivity passes through a maximum as the surface zone is traversed. It is argued that such a maximum is qualitatively consistent with the known sensitivity of the conductivity of liquid mercury to variations in the liquid structure.

I. INTRODUCTION

FOR almost a decade there has been controversy concerning the optical properties of liquid mercury. It is the purpose of this paper to show how this controversy may be resolved, and to examine the implications of that resolution for the methods used to determine the optical properties of a class of liquid metals. Without intending to be pedantic, it is important to start by noting that any analysis of observations requires an established correspondence between the phenomena that theory seeks to explain and those which experiment can actually measure. In optical studies of condensed phases of matter, it is almost universally presumed that such a correspondence exists between the properties of a theoretical, semi-infinite medium, bounded by a geometrical surface, and those of a real, finite medium, bounded by a physical surface. It is further presumed, therefore, that the bulk parameters of the material under study may be deduced directly from careful optical experiments, without regard to any special properties of the surface. The prime contention of the present work is that these presumptions are not necessarily justified.

It should be clear at the outset that many of the conclusions reached in the course of this work are speculative. We do not pretend to have undertaken a rigorous investigation of the properties of real surfaces, nor even to have suggested fruitful lines along which such an investigation might proceed. Rather, we aim simply to demonstrate that there exists a class of substances whose optical properties cannot intelligently be understood without appeal to the nature of the surface.

Throughout this paper we shall be considering the surface of any material as a diffuse transition zone, probably no more than a few atomic layers thick, over which the intensive properties of the system change in a continuous (though not necessarily monotonic) fashion from those of the bulk material to those of a contact medium such as air, vacuum, or an optical window. Clearly, the familiar ideal geometric surface represents the limiting case in which the width of this zone approaches zero.

The material we discuss is divided into theoretical and experimental parts. In Sec. II we examine the solutions to Maxwell's equations describing the interaction of electromagnetic radiation with a conducting medium whose surface is not a geometric boundary. We show that in such a case the optical properties of the system must be influenced by the characteristics of the surface zone, and we attempt to specify the physical conditions necessary for these effects to be measurable. Furthermore, we suggest that such optical phenomena must appear to some degree at nearly all surfaces, but that they should be most pronounced at the surfaces of liquids whose conductivities are, by metallic standards, relatively low. Thus we surmise that as we move down the scale of conductivity, surface contributions to the optical spectrum may become appreciable in the lower portion of the metallic range, and may even dominate the optical properties as we approach the range of transition from metallic to insulating behavior.

If these hypotheses are correct they should certainly apply to the case of liquid mercury, and we shall show that the accumulated experimental evidence in the literature, examined in this light, suggests that they do. To confirm this evidence we present, in Sec. III, new reflection data for liquid mercury in the wavelength

* Present address: Department of Chemistry, The Johns Hopkins University, Baltimore, Maryland 21218.

range 0.5–30 μ. Also described in Sec. III is a versatile and sensitive infrared spectrometer which we have constructed and used in these experiments. The new data obtained may be consistently interpreted as confirming our hypothesis that surface effects do influence the reflection spectrum of liquid mercury.

Section IV presents a speculative discussion, in the light of our results and of recent theoretical treatments, of the kinds of variations that might be expected in the properties of liquid mercury across its surface zone. We construct a rough model for the conductivity profile and calculate the optical properties of such a system, using a product of Herpin matrices for a stratified medium to approximate the analytic solutions of Maxwell's equations. The (possibly) unrealistic choice of parameters necessary to fit these calculated properties to the optical data reflects the crudity of our model, but the final agreement is close enough to indicate that our original hypotheses were probably not unfounded. We conclude that further investigations of the type reported herein should contribute substantially to the understanding, not only of interfacial phenomena as such, but also of the more general characteristics of disordered systems whose properties fall near the threshold of the metallic range.

II. GENERAL COMMENTS

A. Maxwell's Equations in an Inhomogeneous Conductor

There is, of course, nothing new in the concept of a diffuse surface zone, nor in the idea that it should affect the optical properties of a medium. It has been known since the time of Drude[1] and of Lord Rayleigh[2] that when plane-polarized light is incident on the surface of a transparent liquid at the Brewster angle, the reflected light is elliptically polarized to a degree determined by the characteristics of the surface zone. A number of such measurements have been made over the years, revealing minimum zone thicknesses ranging from 3–7 Å for water[3] to more than 1000 Å for critical fluid mixtures.[4] What is surprising is that over the same period of time these effects have been ignored in applying virtually the same experimental method to the determination of the optical properties of conducting media.

Let us consider, then, an isotropic, inhomogeneous, nonmagnetic conductor whose properties are constant in planes perpendicular to the z axis. Let the surface zone be centered about the plane $z=0$. We assume that all macroscopic intensive properties of the system are scalar functions of the coordinate z only and define as positive the z direction in which the conductivity $\sigma(z,\omega)$ tends to its bulk value. Suppose an electromagnetic wave of frequency ω, linearly polarized at an angle θ to the plane $y=0$, propagates in that plane at an angle φ to the z axis. We now make the key assumption, perhaps dubious, that Maxwell's equations will hold over regions as small as the effective width of our transition zone, or that if they do not, they remain approximations sufficiently good that their breakdown can be corrected for by suitable parametrization of our results. It is not at present possible to offer justification for this assumption other than its apparent success in the case of dielectric liquids, as discussed above, and the necessity to have some well-defined starting point for an analysis of the interaction of radiation with the inhomogeneous conductor described.

Under the conditions stated, if $\mathcal{E}(x,z,\omega,t)$ is the electric vector and $\mathcal{H}(x,z,\omega,t)$ is the magnetic vector of the electromagnetic wave, it is necessary that[5]

$$\text{curl}\ \mathcal{E}=-c^{-1}\partial\mathcal{H}/\partial t \tag{2.1a}$$

$$\text{curl}\,\mathcal{H}=c^{-1}[\partial\mathcal{E}/\partial t+4\pi\mathbf{J}(x,z,\omega,t)], \tag{2.1b}$$

where $\mathbf{J}(x,z,\omega,t)$ is the current density. Except under conditions when the anomalous skin effect is important it is also true that

$$\mathbf{J}(x,z,\omega,t)=\sigma(z,\omega)\,\mathcal{E}(x,z,\omega,t). \tag{2.2}$$

We assume that the time dependencies of $\mathcal{E}$ and $\mathcal{H}$ are given by

$$\mathcal{E}(x,z,\omega,t)=\mathbf{E}(x,z,\omega)e^{i\omega t}$$

and

$$\mathcal{H}(x,z,\omega,t)=\mathbf{H}(x,z,\omega)e^{i\omega t}$$

so that Eqs. (2.1a) and (2.1b) become

$$\text{curl}\ \mathbf{E}=-(i\omega/c)\mathbf{H} \tag{2.3a}$$

and

$$\text{curl}\,\mathbf{H}=(i\omega/c)\epsilon(z,\omega)\mathbf{E}, \tag{2.3b}$$

where the complex dielectric constant is given by

$$\epsilon(z,\omega)\equiv 1-4\pi i\sigma(z,\omega)/\omega. \tag{2.4}$$

Following standard procedure, by taking the curl of (2.3a) and the divergence of (2.3b), we can eliminate $\mathbf{H}$ and obtain

$$\nabla^2\mathbf{E}+\text{grad}\left(\mathbf{E}\cdot\frac{\text{grad}\,\epsilon(z,\omega)}{\epsilon(z,\omega)}\right)=-\frac{\omega^2}{c^2}\epsilon(z,\omega)\mathbf{E}. \tag{2.5a}$$

Similarly, eliminating $\mathbf{E}$,

$$\nabla^2\mathbf{H}+\left(\frac{\text{grad}\,\epsilon(z,\omega)}{\epsilon(z,\omega)}\right)\times\text{curl}\,\mathbf{H}=-\frac{\omega^2}{c^2}\epsilon(z,\omega)\mathbf{H}. \tag{2.5b}$$

Equations (2.5) have plane-wave solutions only if the second term on the left-hand side of each is zero,

[1] P. Drude, *Theory of Optics*, translated by C. R. Mann and R. A. Millikan (University of Chicago Press, Chicago, 1902), pp. 287 ff.
[2] Lord Rayleigh, Phil. Mag., **33**, 1 (1892).
[3] K. Kinosita and H. Yokota, J. Phys. Soc. Japan **20**, 1086 (1965). Contains references to earlier measurements.
[4] G. H. Gilmer, W. Gilmore, J. Huang, and W. W. Webb. Phys. Rev. Letters **14**, 491 (1965)

[5] See any standard text on optics; e.g., J. A. Stratton, *Electromagnetic Theory* (McGraw-Hill Book Co., New York, 1941), Chap. 1.

i.e., only if $\epsilon(z,\omega)=\epsilon(\omega)$, a constant in space. Where this is not so, the problem is complicated immeasurably—in fact, there are very few such cases for which the equations can be solved analytically at all.

We can gain some idea of the consequences of retaining the z dependence of ϵ by considering a specific example. A wide variety of possible variations of $\epsilon(z)$ can be approximated by assigning to the conductivity the so-called Epstein profile, introduced by Epstein in a study of the reflection of radio waves from the ionosphere, and by Eckart[6] in a treatment of reflection of electrons from a potential barrier:

$$\sigma(w)=\frac{-w}{1-w}\left(\sigma_b+\frac{\sigma_s}{1-w}\right), \quad w\equiv -e^{z/\Delta}. \tag{2.6}$$

As $z\to\infty$, we have $\sigma(w)\to\sigma_b$, the bulk value of the conductivity, while the "surface term" in σ_s vanishes. As we pass through $z=0$, the bulk term drops monotonically with z, while the surface term passes through an extremum. The profile is sketched in Fig. 1, which is due to Eckart.[6]

A simple separation of variables suffices to show that Eqs. (2.5) have the usual x-dependence $e^{-i(\omega/c)x\sin\varphi}$, so that (2.3) assumes the form

$$\begin{aligned}
&\partial E_y/\partial z=(i\omega/c)H_x,\\
&\frac{\partial H_x}{\partial z}=\frac{i\omega}{c}[\epsilon(z)-\sin^2\varphi]E_y, \qquad (2.7a)\\
&H_z=E_y\sin\varphi\,;\\
&\frac{\partial E_x}{\partial z}=-\frac{i\omega}{c}\left(\frac{\epsilon(z)-\sin^2\varphi}{\epsilon(z)}\right)H_y,\\
&\partial H_y/\partial z=-(i\omega/c)\epsilon(z)E_x, \qquad (2.7b)\\
&E_z=-\frac{\sin\varphi}{\epsilon(z)}H_y.
\end{aligned}$$

As in the case of a homogeneous conductor, these two sets of equations are independent, and can be treated mathematically as characterizing separate waves. Equation (2.7a), of course, represents the transverse electric (TE) component, and (2.7b) the transverse magnetic (TM) component, in the terminology of Born and Wolf.[7] For the tangential components of the TE wave, Eqs. (2.5) are

$$\begin{aligned}
&\frac{\partial^2 E_y}{\partial z^2}=\frac{\omega^2}{c^2}[\epsilon(z)-\sin^2\varphi]E_y, \qquad (2.8a)\\
&\frac{\partial^2 H_x}{\partial z^2}-\frac{\partial \ln[\epsilon(z)-\sin^2\varphi]}{\partial z}\frac{\partial H_x}{\partial z}=\frac{\omega^2}{c^2}[\epsilon(z)-\sin^2\varphi]H_x,
\end{aligned}$$

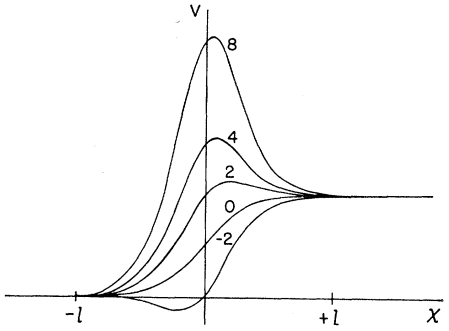

FIG. 1. The Epstein profile, after Eckart (Ref. 6). In Eckart's paper the coordinate x corresponds mathematically to our z, the parameter l to our Δ, and the quantity V to our $\sigma(\omega)$. The numbers labelling each curve are values of the ratio σ_s/σ_b.

and for those of the TM wave

$$\begin{aligned}
&\frac{\partial}{\partial z}\left(\frac{\epsilon(z)}{\epsilon(z)-\sin^2\varphi}\frac{\partial E_x}{\partial z}\right)=-\frac{\omega^2}{c^2}\epsilon(z)E_x,\\
&\frac{\partial}{\partial z}\left(\frac{1}{\epsilon(z)}\frac{\partial H_y}{\partial z}\right)=-\frac{\omega^2}{c^2}\epsilon(z)H_y.
\end{aligned} \tag{2.8b}$$

At normal incidence ($\varphi=0$), the two sets of equations become identical, and can be solved in the case of the Epstein profile. The equation for E is then an example of Riemann's P-equation,[8] and will in general have 24 hypergeometric solutions, of which we can choose the appropriate ones by demanding, as boundary conditions, convergence to plane-wave forms at infinity. The solution for H is then obtained directly from (2.7).

For oblique incidence, the TE system can, obviously, also be solved in this way. Instead of plane waves, we obtain for the electric vector in the inhomogeneous medium

$$\begin{aligned}
&E_y(x,z,\omega)\\
&=E_0e^{-i(\omega/c)x\sin\varphi}(1-w)^\beta\left(\frac{w}{w-1}\right)^\alpha\\
&\qquad\times F\left(U,V,W;\frac{1}{1-w}\right) \qquad (2.9a)
\end{aligned}$$

and for the magnetic vector:

$$\begin{aligned}
&H_x(x,z,\omega)\\
&=(\epsilon_b-\sin^2\varphi)^{1/2}E_0e^{-(i\omega/c)x\sin\varphi}(1-w)^\beta\left(\frac{w}{w-1}\right)^\alpha\\
&\times\left[\left(\frac{\alpha+\gamma}{w-1}-\frac{\alpha}{w(w-1)}\right)F\left(U,V,W;\frac{1}{1-w}\right)\right.\\
&\left.\qquad+\frac{U}{1-w}F\left(U+1,V,W;\frac{1}{1-w}\right)\right]. \qquad (2.9b)
\end{aligned}$$

[6] P. S. Epstein, Proc. Natl. Acad. Sci. (U. S.) **16**, 627 (1930), C. Eckart, Phys. Rev. **35**, 1303 (1930). The full mathematical treatment for normal incidence was presented almost simultaneously, and, it seems, independently by the two authors, but earlier presentations of special cases had been made in lectures by Epstein (see Eckart's footnote 4).

[7] M. Born and E. Wolf, *Principles of Optics* (Pergamon Press, Inc., New York, 1965), 3rd ed., pp. 52 ff.

[8] See, e.g., E. T. Whitaker and G. N. Watson, *A Course of Modern Analysis* (Cambridge University Press, Cambridge, 1927), 4th ed., pp. 206 and 283 ff.

Here w is defined as in (2.6), ϵ_b is the bulk dielectric constant, $\epsilon_b=1-4\pi i\sigma_b/\omega$, F is the hypergeometric function, $U\equiv\alpha-\beta+\gamma$, $V\equiv\alpha-\beta+1-\gamma$, and $W\equiv 1-2\beta$, where

$$\alpha\equiv -(i\omega\Delta/c)\sin\varphi,$$
$$\beta\equiv -(i\omega\Delta/c)(\epsilon_b-\sin^2\varphi)^{1/2}, \tag{2.10}$$

and

$$\gamma\equiv\tfrac{1}{2}+(c^2-16\pi i\omega\sigma_s\Delta^2)^{1/2}/2c.$$

Our notation and choice of parameters differ slightly from those of Eckart.[6] After some labor along the lines he sketches, we obtain for the amplitude reflection coefficient r_s for light polarized perpendicular to the plane of incidence, the relation

$$r_s=\frac{\Gamma(1-\beta-\alpha-\gamma)\Gamma(-\beta-\alpha-\gamma)\Gamma(2\alpha)}{\Gamma(-\beta+\alpha+\gamma)\Gamma(1-\beta+\alpha+\gamma)\Gamma(-2\alpha)}. \tag{2.11}$$

As $\Delta\to 0$, this reduces to the usual expression[9]

$$r_s\to\frac{-\beta+\alpha}{-\beta-\alpha}=\frac{\cos\varphi-(\epsilon_b-\sin^2\varphi)^{1/2}}{\cos\varphi+(\epsilon_b-\sin^2\varphi)^{1/2}}. \tag{2.12}$$

To obtain the amplitude reflection coefficient r_p for light polarized parallel to the plane of incidence, and hence the full set of optical properties, it is necessary to solve the set of equations for the TM component. However, examination of Eq. (2.7b) after change in variable from z to w reveals that both contain irregular singular points, and we are not able to solve them directly. We shall return to this problem in Sec. IV, where we introduce numerical methods that enable us to study the effects of a given profile quantitatively.

In this section, our purpose is simply to show that the presence of a surface transition layer of finite width can change markedly the solutions of Maxwell's equations as compared to the solutions for a conductor with a geometric surface. The magnitude of the deviations from sharp-boundary solutions depends directly upon the effective width 2Δ of the transition zone, and, in the case of the Epstein profile, upon the magnitude of the surface conductivity parameter σ_s. When these are large enough for the complex quantity γ to differ appreciably from unity, the relation between the real and imaginary parts of r_s will be affected somewhat more than will its absolute value. If this is also true for r_p, we can anticipate some difference between the results of ellipsometric determinations of the optical properties and those of absolute measurements of the reflectivity. The effect described would be the direct analog of the phase change across the transition zone[10] which is responsible for the ellipsometric properties of transparent liquids mentioned above.

[9] See, e.g., A. V. Sokolov, *Optical Properties of Metals* (Blackie and Son Ltd., London, 1967), pp. 28–29.

[10] Reference 1, p. 289.

In the case of a conductor, however, there is no way of distinguishing between this phase change and that due to the bulk-value absorption coefficient. Thus, there will be errors if the usual sharp-surface ellipsometric formulas for the optical properties are naively applied to describe observations of an inhomogeneous system. Ellipsometric determinations are notoriously sensitive to such errors, as recent calculations of the effect of thin contaminating dielectric films on metal surfaces suggest; we discuss these calculations below. (Again, it is curious that so many of the experimental arguments over the optical properties of liquid metals should have concentrated on the possible effect of foreign thin, homogeneous, transparent layers, while the effect of the natural thin, inhomogeneous, absorbing layer has been all but ignored.)

The effect of a surface zone on, say, the reflectivity at normal incidence is much less pronounced. Even in absolute reflectivity measurements, however, the form of r_s suggests that the dependence on the angle of incidence will be different from its form in the conventional Fresnel expressions. Similar effects on the absolute reflectivity have been calculated by Burge and Bennett[11] in their studies of contaminating films.

B. Liquid Metals: Surface Effects in Good Conductors

Having established, qualitatively, that an inhomogeneous surface zone may affect the optical properties of a conductor, let us turn to the question of which real physical systems are most likely to display such an effect prominently.

It is now well established[12] that the electrical properties of most liquid metals are in remarkable agreement with the nearly-free-electron (NFE) theory of Ziman,[13] and of Bradley *et al.*[14] According to this theory, the conduction electrons are in plane-wave states weakly perturbed by a small ionic pseudopotential. The cross section for scattering due to the pseudopotential is determined in the Born approximation, and this scattering leads to an electronic relaxation time τ_z, given by

$$\frac{1}{\tau_z}=\frac{m^*}{12\pi^2\hbar^3N}\int_0^{2K_F}a(K)\,|\tilde{u}_K|^2K^3\,dK, \tag{2.13}$$

where N is the density of conduction electrons of effective mass m^*, $a(K)$ is the liquid structure factor, and $\tilde{u}_K$ is the Kth Fourier component of the pseudopotential. The electronic mean free path Λ is then given directly by

$$\Lambda=v_F\tau_z, \tag{2.14}$$

where v_F is the velocity of electrons at the Fermi surface.

[11] D. K. Burge and H. E. Bennett, J. Opt. Soc. Am. **54**, 1428 (1964).

[12] For reviews, see, e.g., (a) N. E. Cusack, Rept. Progr. Phys. **26**, 36 (1963); (b) N. F. Mott, Advan. Phys. **16**, 49 (1967).

[13] J. M. Ziman, Phil. Mag. **6**, 1013 (1961).

[14] C. C. Bradley, T. E. Faber, E. G. Wilson, and J. M. Ziman, Phil. Mag. **7**, 865 (1962).

When an electromagnetic field of frequency ω is applied to the liquid metal, the electronic states are perturbed by the field and, of course, by the weak scattering described above. In the steady state the distribution of electrons is described by a Boltzmann equation.[15] If f_0 is the equilibrium Fermi distribution function in the absence of a field and $f_1(\mathbf{v},\mathbf{k})$ is the change in the distribution function due to the perturbation, f_1 is found to satisfy (approximately)

$$\frac{1+i\omega\tau_z}{\tau_z v_z} f_1 + \frac{\partial f_1}{\partial z} = \frac{\epsilon}{m v_z} \frac{\partial f_0}{\partial v_y} E(z). \tag{2.15}$$

Neglect of the second (diffusion) term on the left-hand side of (2.15) leads directly[16] to the classical Drude[17] relation for the conductivity,

$$\sigma(\omega) = \sigma_0/(1+i\omega\tau_z), \tag{2.16}$$

where the dc conductivity is given by

$$\sigma_0 = Ne^2\tau_z/m^*. \tag{2.17}$$

One condition on the validity of (2.16), then, is that neglect of the diffusion term in (2.15) be justified. Reuter and Sondheimer[18] have shown that this condition holds only if

$$\delta \equiv \frac{c}{(2\pi\omega\sigma_0)^{1/2}} \gg \frac{\Lambda}{(1+\omega^2\tau_z^2)^{3/4}}, \tag{2.18}$$

where δ is the classical penetration depth of a plane wave into the metal surface. Clearly, this relation does not hold at frequencies such that $\omega\tau_z \gg 1$. We are then in the region of the anomalous skin effect: The electron mean free path is much longer than the field penetration depth, and so the electron is effectively perturbed by the field over only a fraction of its mean free path. In good conductors, where the mean free path is of the order of 10–50 interatomic distances, the anomalous skin effect begins at frequencies as low as those corresponding to the far infrared.[19]

Reuter and Sondheimer explored the consequences of retaining the diffusion term in (2.15). They arrived at an integro-differential equation whose solution depends on the boundary conditions on electrons reflected from the surface. Their results, which have been simplified by Dingle,[19] depend on a parameter p, which varies between zero and one according to whether the electron reflection from the surface is diffuse or specular.

The point is that under conditions such that the anomalous skin effect is important, it should not be possible to measure any transition zone effect. The surface zone width is likely to be no more than a small fraction of the bulk mean free path, so that the electron will see it only as a slightly smeared out surface. The smearing may affect slightly the characteristics of reflection of the electron from the surface, but we speculate that these variations can be subsumed into the usual empirical adjustment of the parameter p in the anomalous skin effect calculation.

C. Metal-to-Insulator Transition: Surface Effects in Poor Conductors

Consider a crystalline metal in which the internuclear separation is gradually increased. Corresponding to the decrease in the density of the electron gas the screening of the Coulomb interaction between electrons and ions decreases until there is no longer effective screening and bound states are created. If the interelectronic repulsion is enough larger than the kinetic energy of the electrons, these states are occupied and the material becomes an insulator, despite the existence of an electron band only partially full. Such insulating states are often found among metallic oxides[20] and valence semiconductors with metallic impurities. This metal-to-insulator transition, studied first by Mott[21] as an extension of the early hypothesis of Wigner,[22] is predicted to occur discontinuously[23] at a specific interatomic distance in a regular lattice free of impurities.

If the metal is molten, however, the absence of a periodic lattice implies that the transition would occur not discontinuously, but gradually over some density range. Mott[12] envisions this region as characterized by increasingly strong electron-ion interactions, a decrease in the mean free path, and a corresponding drop in the density of states $n(\epsilon_F)$ at the Fermi level. When this drop is sufficiently large, he theorizes that the theorem of Edwards[24] that $n(\epsilon_F)$ does not appear in the conductivity expression must break down, so that the dc conductivity diminishes and the ac conductivity shifts toward the Lorentzian form[25] characteristic of localized states:

$$\sigma_{\text{loc}}(\omega) = \frac{i\sigma_0\omega\gamma}{(\omega_0^2-\omega^2)+i\omega\gamma}. \tag{2.19}$$

In Eq. (2.19), the ac conductivity corresponding to the localized states is centered about ω_0, with half-width γ.

Mott estimates that these localized states should appear when Λ approaches the Fermi wavelength and the interatomic distance. This is apparently the case in liquid tellurium, for which Hodgson's[26] optical data

[15] See, e.g., J. M. Ziman, *Electrons and Phonons* (Oxford University Press, Oxford, 1960), pp. 264 ff.
[16] J. M. Ziman, *Principles of the Theory of Solids* (Cambridge University Press, Cambridge, 1964), p. 238.
[17] Reference 1, pp. 396 ff.
[18] G. E. H. Reuter and E. H. Sondheimer, Proc. Roy. Soc. (London) **A195**, 336 (1948).
[19] R. B. Dingle, (a) Physica **18**, 985 (1952); (b) **19**, 311 (1953); (c) **19**, 729 (1953).
[20] See, e.g., F. J. Morin, Phys. Rev. Letters **3**, 34 (1959).
[21] N. F. Mott, Proc. Phys. Soc. (London) **62**, 416 (1949).
[22] E. Wigner, Trans. Faraday Soc. **34**, 678 (1938).
[23] But cf. N. F. Mott and E. A. Davis, Phil. Mag. **17**, 1269 (1968).
[24] S. F. Edwards, Proc. Roy. Soc. (London) **A267**, 518 (1962).
[25] Reference 9, pp. 66 ff.
[26] J. N. Hodgson, Phil. Mag. **8**, 735 (1963).

show a superposition of Drude and Lorentzian forms. Mott[27] originally speculated that it could also be the case in liquid mercury, and used this hypothesis to attempt to explain the abnormal electrical properties of this metal. The weight of the evidence, as Mott[12] himself has now summarized it, seems to be against this conclusion, and Mott[12] has found that he can explain most of the abnormalities equally well in terms of the structural properties that we shall discuss in a later section.

In any case, liquid mercury clearly does not lie much above the lower end of the metallic range ($\sigma_0 = 9.35 \times 10^{15}$ esu, $\Lambda \sim 7$ Å, interatomic distance ~ 3 Å, $\lambda_F \sim 5$ Å), and we can again inquire into the surface effects to be expected. For liquid Hg there is no measurable anomalous skin effect, and the classical penetration depth δ is 10 to 50 times the interatomic distance. Thus, an electromagnetic wave must penetrate throughout and beyond the range of the surface transition zone. More important, the small value of Λ implies that the conduction electron sees nearly every ion, and hence the conductivity has become comparatively structure-sensitive. An optical measurement has, in short, become a sort of electron-diffraction experiment, and should be responsive to the characteristics of the surface zone.

D. Disputed Optical Constants of Liquid Mercury

Mercury is the metal most commonly available in the liquid state, and its optical properties have been measured in over a dozen different laboratories[28] since the early work of Drude.[29] Most of the measurements have been based on ellipsometry, and most of them have yielded optical constants significantly higher than those derived from the simple Drude expression (2.16). The first really extensive and precise work was performed by Schulz,[28] who measured both the absolute reflectivities at 45° incidence of interfaces between mercury and several different dielectrics, and the phase change on reflection at normal incidence using reflection interference filters. Both his sets of results agreed with the predictions of the Drude theory to within a remarkable precision.

Schulz's data were almost immediately contradicted by the ellipsometric work of Hodgson,[30] who measured free surfaces and found optical constants $\sim 20\%$ higher than the Drude values. Since Hodgson's surfaces had been exposed to air, while Schulz had taken great pains to protect his surfaces, it was widely assumed[31] that Schulz's results were correct. This conclusion was reinforced by the low-energy results of Wilson and Rice,[32] who measured the reflectivity at near-normal incidence for free surfaces under vacuum.

Meanwhile, Lelyuk[33] and co-workers had determined, from ellipsometric measurements, optical constants even higher than those of Hodgson, and soon Faber and Smith,[34] using a new ellipsometer whose ingenious design eliminated most of the usual errors in polarizer settings, had substantially confirmed Hodgson's results. From their account of the work, it is possible to infer that Faber and Smith also avoided most of the other sources of experimental error common to ellipsometric determination.

First, they repeated their measurements at several angles of incidence with negligible effect on the results. Smith and Stromberg[35] have shown theoretically that such behavior is likely to indicate freedom from any significant errors due to window birefringence and/or misalignment of the ellipsometer, and they are able to account for the angular dependence reported earlier by Tronstad and Feachem[36] in terms of these errors. Invariance of the measured optical constants with angle of incidence does not, however, provide any indication that the surface under study is free from contamination. Burge and Bennett[11] have demonstrated that thin dielectric films deposited on conducting surfaces can affect the apparent optical constants enormously without producing any measurable angular dependence, and this conclusion has been confirmed for the case of contaminated mercury by Smith and Stromberg[35] and, independently, by Faber and Smith[34b] themselves. (This is not inconsistent with the surface profile effect calculation in Sec. IV. The angular dependence of the ellipsometric properties predicted by our results is also negligible over the range of angles of incidence where ellipsometric measurements are experimentally feasible. The absolute reflectivity, however, varies considerably in this range, in a way that is qualitatively different from that expected for reflection from sharp surfaces. See Sec. IV for an amplification of this point.)

Both thin-film calculations do show, however, that in the particular instance of a free mercury surface, the effect of an oxidelike layer would be to force the measured optical constants downward, toward the Drude values. Faber and Smith used an argon glow discharge to clean their surfaces, and measured the change in apparent optical constants as the newly cleaned mercury was allowed to stand. They obtained close agreement with the theoretical contamination curves.

We are not clear as to whether the glow-discharge procedure is a cleansing or a dirtying process, nor on

[27] N. F. Mott, Phil. Mag. **13**, 989 (1966).
[28] For early references, see L. G. Schulz, J. Opt. Soc. Am. **47**, 64 (1957).
[29] P. Drude, Ann. Physik **39**, 530 (1890).
[30] J. N. Hodgson, Phil. Mag. **4**, 189 (1959).
[31] See, e.g., T. E. Faber, in *Optical Properties and Electronic Structure of Metals and Alloys*, edited by F. Abelès (North-Holland Publishing Co., Amsterdam, 1966), p. 259.
[32] E. G. Wilson and S. A. Rice, Phys. Rev. **145**, 55 (1966).
[33] L. G. Lelyuk, I. N. Shklyarevskii, and R. G. Yarovaya, Opt. i Spektroskopiya **16**, 484 [English transl.: Opt. Spectry. (USSR) **16**, 263 (1964)].
[34] (a) N. V. Smith, Advan. Phys. **16**, 629 (1967); (b) T. E. Faber and N. V. Smith, J. Opt. Soc. Am. **58**, 102 (1968).
[35] L. E. Smith and R. R. Stromberg, J. Opt. Soc. Am. **56**, 1539 (1966).
[36] L. Tronstad and C. G. P. Feacham, Proc. Roy. Soc. (London) **A145**, 115 (1934).

how much scattered light was introduced by the transmission grating used in this experiment. Nevertheless, what makes these results convincing in our eyes is their almost exact agreement with the single wavelength ellipsometric measurement of Smith,[37] the only worker on this problem who has actually demonstrated the cleanliness of his surfaces by measurement of surface tension, contact potential, etc.

The difficulty we now face is that the results of Schulz are equally convincing. It is scarcely conceivable that the techniques used by Schulz for forming his interfaces could have led to a contaminating layer at all, and still more unlikely that any such layer would be capable of producing the same error for both his methods of measurement. It is an even stranger coincidence that this error should produce exact agreement with Drude values. Moreover, Boiani and Rice,[38] using an improved version of the spectrometer of Wilson and Rice, have recently extended their normal incidence reflectivity measurements under both vacuum and helium atmosphere, and have found that agreement with the Drude curve is preserved to wavelengths of at least 8500 Å.

We have no basis, then, for choosing between the two sets of results on experimental grounds, and we have next to ask whether there is a case for choosing between them theoretically. Since the real part of the conductivity must return to the electrically measured dc value σ_0, Hodgson's work implies that $\omega\epsilon_2$ must pass through a maximum in the infrared. Faber[39] has attempted to establish the necessity of the resulting increase in the area under the curve $\omega\epsilon_2(\omega)$ in terms of the sum rule

$$\frac{2m^*}{\pi e^2}\int_0^\infty \omega\epsilon_2(\omega)d\omega = N, \tag{2.20}$$

where N is the total electron density. The effect is sketched in Fig. 2.[40,41] The contribution from the Drude curve must necessarily sum to N_c, the number density of conduction electrons, and Faber argues that this sum must be augmented if coupling with the d bands is properly taken into account. The effect is simply an extension of the well-known[42] enhancement of oscillator strengths for transitions of outer valence electrons in atoms, at the expense of core electrons.

We accept this argument in principle, but doubt that it can be made quantitative by dubious extrapolations of d-band absorption edges, as Faber asserts. We would need some better estimate of the magnitude of the coupling, and of the compensatory effect of upward transitions and of excitations such as the Hopfield[43] resonance seen by Wilson and Rice, before we can predict whether the effect would be measurable at all.

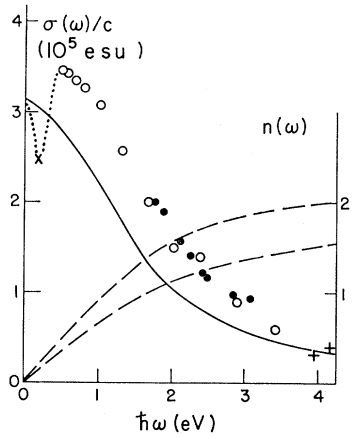

FIG. 2. Conductivity of liquid mercury as a function of frequency, after Faber (Ref. 31). In Faber's notation, $\sigma(\omega)$ is just $\omega\epsilon_2(\omega)$. The solid curve displays the predictions of the Drude free electron theory, while the points give the ellipsometric results of several workers: ●, Hodgson (Ref. 30); ○, Faber and Smith (Ref. 34); +, O'Brien (Ref. 40); ×, Beatty and Conn (Ref. 41). The lower and upper dashed lines represent the area $n(\omega) = (2m/\pi e^2)\int_0^\omega \omega\epsilon_2(\omega)d\omega$ [see Eq. (2.20)] as calculated from the Drude and experimental curves, respectively. As $\omega\to\infty$, $n(\omega)$ given by the lower curve approaches 2.0, while $n(\omega)$ given by the upper curve approaches ~2.6.

In any event, the argument says nothing at all about the actual source of the Hodgson maximum, although Hodgson himself[44] has attempted to explain it in terms of Mott's original low-density-of-states hypothesis. Certainly neither the corrections to Ziman's theory proposed by Faber[39] nor the independent treatment of the problem by Helman and Baltensperger[45] lead to behavior of this form.

We are left, then, with two apparently contradictory sets of confirmed data, and with no theoretical grounds for choosing between them. We have no choice but to entertain the possibility that both sets are correct. From our point of view, of course, the Hodgson results, in conjunction with those of Schulz, suggest the sort of surface transition zone effect for which, as we have seen, conditions in liquid mercury are ripe. Perhaps the most severe test of this hypothesis is afforded by absolute reflectivity measurements on the low-energy side of the Hodgson conductivity maximum. If the maximum is a "real" property of bulk mercury, we would expect a sharp change in the slope of the reflectivity as the conductivity decreases rapidly to its dc value; if the maximum is a surface phenomenon, the effect should be much less pronounced, if measurable at all. Except for one experimental run by Schulz,[28] no reliable reflection or ellipsometric studies have been extended far enough into the infrared to see either the maximum itself, or the absorption edge associated with it, if one exists.

[37] T. Smith, J. Opt. Soc. Am. **57**, 1207 (1967).
[38] J. Boiani and S. A. Rice, preceding paper, Phys. Rev. **185**, 933 (1969).
[39] T. E. Faber, Advan. Phys. **15**, 547 (1966).
[40] B. O'Brien, Phys. Rev. **27**, 93 (1926).
[41] J. R. Beatty and G. K. Y. Conn, Phil. Mag. **46**, 222 (1955).
[42] See, e.g., U. Fano and J. W. Cooper, Rev. Mod. Phys. **40**, 441 (1968).
[43] J. Hopfield, Phys. Rev. **139**, A419 (1965).
[44] J. N. Hodgson, Advan. Phys. **16**, 675 (1967).
[45] J. S. Helman and W. Baltensperger, Physik Kondensierten Materie **5**, 60 (1966).

To carry out such a measurement requires an instrument of extraordinary sensitivity, since both ellipsometric[46] and reflectivity[32] measurements grow more insensitive to the optical constants as the wavelength increases. We have constructed such an instrument, designed for near-normal reflectivity measurements in the infrared on a wide variety of materials. In Sec. III we describe this device and present reflectance data for liquid mercury in the wavelength range 0.5–30 μ.

III. EXPERIMENTAL MEASUREMENTS

A. General Considerations in Instrument Design

In seeking to construct our infrared spectrometer we encountered first the question of whether we could hope to profit more from ellipsometric or direct reflection measurements on the systems of interest to us. In the absence of surface transition zone effects the two procedures should serve as equivalent methods for determination of the optical constants, $n(\omega)$ and $k(\omega)$, characteristic of the system at a given frequency ω. These are defined as the real and imaginary parts of the complex index of refraction,

$$\mathfrak{N}(\omega)\equiv n(\omega)-ik(\omega), \tag{3.1}$$

and are related to the complex dielectric constant of Eq. (2.3) by the definition

$$\epsilon(\omega)\equiv\mathfrak{N}^2(\omega). \tag{3.2}$$

Alternatively, the optical properties may be conveniently represented in terms of the real and imaginary parts of $\epsilon(\omega)$,

$$\epsilon_1=n^2-k^2;\quad \epsilon_2=2nk, \tag{3.3}$$

where ϵ_1 and ϵ_2 are defined by Eq. (2.4). For light of frequency ω incident upon an isotropic specimen at an angle of incidence φ, these quantities determine the amplitude reflection coefficients, r_s and r_p, for the components of the light polarized perpendicular and parallel to the plane of incidence, respectively. If sharp-surface boundary conditions are applied to the Maxwell equations (2.5) at an interface of the sample with a contact medium of refractive index $\mathfrak{N}_0=n_0-ik_0$, these expressions are found to be[47]

$$r_s=\frac{(\mathfrak{N}_0^2-\mathfrak{N}_0^2\sin^2\varphi)^{1/2}-(\mathfrak{N}^2-\mathfrak{N}_0^2\sin^2\varphi)^{1/2}}{(\mathfrak{N}_0^2-\mathfrak{N}_0^2\sin^2\varphi)^{1/2}+(\mathfrak{N}^2-\mathfrak{N}_0^2\sin^2\varphi)^{1/2}}, \tag{3.4a}$$

$$r_p=\frac{\mathfrak{N}_0^2(\mathfrak{N}^2-\mathfrak{N}_0^2\sin^2\varphi)^{1/2}-\mathfrak{N}^2(\mathfrak{N}_0^2-\mathfrak{N}_0^2\sin^2\varphi)^{1/2}}{\mathfrak{N}_0^2(\mathfrak{N}^2-\mathfrak{N}_0^2\sin^2\varphi)^{1/2}+\mathfrak{N}^2(\mathfrak{N}_0^2-\mathfrak{N}_0^2\sin^2\varphi)^{1/2}}. \tag{3.4b}$$

The ellipsometric method determines n and k from these quantities through direct measurement of the real and imaginary parts of the complex ratio r_s/r_p, while reflectance experiments yield the same information through various combinations of the energy reflection coefficients $R_s=r_s^*r_s$ and $R_p=r_p^*r_p$.[48]

For most purposes, ellipsometric measurements offer somewhat greater sensitivity, particularly in the metallic region, where, as we shall see presently, large changes in the optical constants generally produce relatively small changes in the absolute reflection coefficients. On the other hand, the sources of experimental error inherent in ellipsometry are apt to be considerably more serious than those characteristic of reflectometry.

We have mentioned several of these disadvantages in Sec. II, and we have no reason to expect that they would not apply to our studies. Indeed, some of them would, if anything, be compounded. For example, polarizers for use in the infrared are available,[49] but do not in general appear to be of the uniformly high quality necessary for precise measurements over a wide range of wavelengths. In view of the great sensitivity of the ellipsometric method to errors in zero polarizer settings,[50] we might anticipate that results obtained using such devices would be open to question.

Furthermore, the employment of ellipsometric techniques would render our work susceptible to the usual difficulties of surface contamination,[11,34b] window birefringence,[35] slight misalignments of the ellipsometer,[35] and the changes in polarization that accompany reflection from any mirrors used in the optical system. It is, to be sure, also true that absolute measurements of R_s and R_p at oblique incidence[48] are subject, more or less, to most of these same sources of error. But a different situation entirely arises as we approach the special case of normal incidence, $\varphi=0$.

A glance at Eqs. (3.4) reveals that in this limit the expressions for r_s and r_p become identical, leading to the familiar expression for the energy reflection coefficient at normal incidence, R_N:

$$R_N=\left|\frac{\mathfrak{N}^2-\mathfrak{N}_0^2}{\mathfrak{N}^2+\mathfrak{N}_0^2}\right|=\frac{(n-n_0)^2+(k-k_0)^2}{(n+n_0)^2+(k+k_0)^2}. \tag{3.5}$$

The plane of incidence and hence the polarization are no longer defined, and nearly all the sources of error encountered in ellipsometric work vanish. The principal exception is surface contamination, and even this, as we shall see shortly, need not be bothersome in our applications.

But despite its relative freedom from experimental error and its obvious simplicity, the normal incidence technique has not found wide favor in optical studies of metals. Some of the reasons for this are probably historical—ellipsometric methods date back to Drude[29]

[46] This is readily apparent from the curves given by I. Simon, J. Opt. Soc. Am. **41**, 336 (1951).

[47] For a clear, detailed derivation, see Ref. 9, Chap. 1.

[48] A summary of these methods is presented by J. Fahrenfort, in Proceedings of the Tenth International Colloquium on Spectroscopy, University of Maryland, 1962, p. 437 (unpublished).

[49] See, e.g., Instructions for Infrared Polarizer, Perkin-Elmer Corp. Report No. 127-1164, 1963 (unpublished).

[50] See, e.g., R. Emberson, J. Opt. Soc. Am. **26**, 443 (1936).

—but some are based on three fundamental limitations inherent in studies at normal incidence. We shall examine these in turn.

First and most obvious, reflectivity measurements at true normal incidence are not experimentally feasible in most optical systems, since they would require that the light source, sample, and detector all be collinear. We are forced, rather, to use Eq. (3.5) as an approximation to the reflectivity (at some arbitrary polarization) measured at a small, but nonzero, value of the angle of incidence. From Eqs. (3.4), we see that this approximation will be adequate so long as $\sin^2\varphi$ remains small compared with n^2 and n_0^2. Wilson and Rice[32] have shown that for a vacuum-liquid mercury interface at $\varphi=10°$ the error introduced in this way is practically always negligible, and is certainly so at long (i.e., visible and infrared) wavelengths.

The second drawback is more serious, and arises from the relative insensitivity of R_N to changes in the optical constants of metals in the infrared region. The extent of this difficulty becomes apparent when we realize that for high values of the ac conductivity $\sigma(\omega)$, the first term in Eq. (2.4) for the complex dielectric constant can be neglected in comparison with the second, and Eqs. (3.2) and (3.1) lead to values of $n(\omega)$ and $k(\omega)$ which are large and approximately equal:

$$n(\omega)\sim k(\omega)\sim[2\pi\sigma(\omega)/\omega]^{1/2}. \tag{3.6}$$

Under these circumstances Eq. (3.5) approaches the familiar Hagen-Rubens[51] relation

$$R_N\sim 1-2\left(\frac{\omega}{2\pi\sigma(\omega)}\right)^{1/2}\sim 1-2\left(\frac{\omega}{2\pi\sigma_0}\right)^{1/2}. \tag{3.7}$$

Then even for reflectivities as low as, say, 80%, a 10% decrease in $\sigma(\omega)$ will bring about no more than a 1% change in the reflectivity—a change which is within the range of experimental error of work such as that of Wilson and Rice.[32] For liquid mercury, such conditions hold for wavelengths greater than $10\,\mu$, but approximate the situation down to the vicinity of $1\,\mu$.[52]

There are at least three approaches toward overcoming this limitation. One is to return to oblique-incidence techniques such as ellipsometry, with some improvement in sensitivity, but with the attendant increase in risk of systematic error. Another is to introduce modulation methods to obtain spectral derivatives; these are extremely responsive to small changes in the optical constants, but are at best of only marginal use in determining their absolute values. The third alternative is simply to construct, carefully and systematically, a straightforward infrared reflectance spectrometer sensitive and stable enough to measure variations in R_N as small as those we have just discussed.

We can immediately define the gross characteristics of such a device. First, we expect that the optical phenomena in which we are interested, such as the Drude absorption, will extend over a considerable range of wavelengths, but that their spectra, especially in these disordered systems, will not be finely structured. We do not, therefore, require the high resolution afforded by a grating monochromator: our needs should be well served by a prism instrument, capable of scanning continuously and extensively at appropriate speeds without benefit of the sort of tedious filter or foreprism adjustments necessary when gratings are used.

Second, we can distinguish our monochromatic light beam from background radiation, from emission from high-temperature samples, and from most scattered light by placing a chopper in the optical path; the ac detector signal produced by the chopped light can be amplified with high selectivity by good quality, low noise lock-in electronics. We note that the chopper frequency must be as low as possible to minimize vibration and mechanical wear, but that it must remain high enough to permit tuning of the lock-ins with reasonable time constants. It must not, of course, be a subharmonic of 60 cps.

The advantages of a light chopper and lock-in amplification cannot be realized, however, unless our detectors themselves are of similarly high quality. We require not only great sensitivity, but low impedance to minimize Johnson noise, and practically zero drift. In addition, to accommodate the extreme variation in light intensity that accompanies the large wavelength changes and wide variety of optical properties with which we are concerned, we seek detectors of maximum linearity and blackbody frequency response. In theory and to a remarkable degree in practice, all these needs are met by thermocouple detectors.[53]

Furthermore, thermocouple devices present no danger of saturation due to background radiation, even when this radiation includes undispersed emission from heated samples. Ideally, a perfect thermocouple junction, isolated *in vacuo*, remains linear up to infinite levels of energy flux; practically, a real thermocouple is limited by its own heat capacity and the thermal conduction of its electrical leads.[54] A simple calculation, based upon the blackbody radiation law and the everyday performance characteristics of thermocouple detectors manufactured by the Perkin-Elmer Corp., reveals that these detectors would remain linear even if our sample were a black body heated to 1000°C.

Finally, it is clear that the sensitivity we require would be all but wasted in a conventional single-beam spectrometer. The operation of such instruments depends on consecutive measurements of the intensity of light reflected from the sample and from some sort of standard reflector. If at a given wavelength the

[51] E. Hagen and H. Rubens, Ann. Physik **14**, 936 (1904).

[52] According to the calculations of Schulz (Ref. 28) who, for obscure reasons, refers to the Hagen-Rubens approximation as the "classical skin effect."

[53] See, e.g., G. K. T. Conn and D. G. Avery, *Infrared Methods* (Academic Press Inc., New York, 1963), pp. 80 ff.

[54] See Ref. 53, p. 82.

reflectivity of the sample is R' and that of the standard is R, these intensities are, respectively,

$$I'=I_0AGR'$$

and

$$I=I_0AGR, \tag{3.8}$$

where I_0 is the intensity of light entering the monochromator, A is the transmission of the atmosphere, and G is the product of the reflection and transmission coefficients of the optical components, the responsivity of the detector, and the electronic gain.

The ratio I'/I will not be a direct measure of the ratio R'/R unless the other factors are all constants in time. The problem is, of course, that in general they are not. Light sources useful in the far infrared are usually small, windowless, high-temperature blackbody radiators. Even with carefully regulated power supplies, they are subject to intensity fluctuations induced by convection cooling in random air currents, by changes in surface composition due to sublimation, oxidation, and decomposition, and by gradual deterioration of the electrical contacts, which are subject to large temperature gradients. These phenomena can and often produce considerable variables in I_0 between the measurements of the sample and the "blank." Moreover, unless the atmosphere can be so well controlled that random variations in humidity and carbon dioxide concentration are precluded throughout the optical path, similar variations, over large segments of the infrared spectrum, will occur in A.

These difficulties, together with some of the effects upon G of electronic drift, can be eliminated by the employment of a split-beam arrangement which allows direct measurement of the intensity ratio I'/I. The intensities measured in the two channels are now

$$I'=I_0A'B'G'R'$$

and

$$I=I_0ABGR, \tag{3.9}$$

where B' and B are the appropriate properties (e.g., reflection or transmission coefficients) of the beam splitter. In the intensity ratio, I_0 cancels immediately, and we recognize that the two optical path lengths can be made close enough that A'/A is always negligibly different from unity. Our ratio I'/I is now constant in time and hence reproducible, but we will have attained this precision at the expense of accuracy in R'/R unless we can compensate for the effect of the beam-splitter spectrum B'/B, and of optical-electronic channel mismatch G'/G. This is easily accomplished by repeating the experiment with a second standard reflector R'' in place of the sample. Dividing the intensity ratio I'/I by I''/I, we obtain cleanly the ratio R'/R'', independent of any extraneous characteristics of the system. The net effect of this "ratio-or-ratios" technique, then, is to combine the accuracy (in terms of the standard reflector R'') of the conventional single-beam sample-in-sample-out procedure with the precision of a careful double-beam experiment.

We have still to deal with the third important disadvantage of reflectivity measurements at normal incidence: the information content of Eq. (3.5) itself. The expressions (3.4), or appropriate combinations of them or their absolute values, comprise a set of two independent equations which can be solved simultaneously for unknown values of the two variables n and k. But at normal incidence this set has become degenerate, and (3.5) represents a single equation in two unknowns. The usual method of attacking this difficulty is by recognizing that R_N represents the squared modulus of the complex amplitude reflection coefficient at normal incidence,

$$r_N=\frac{n-ik-\mathfrak{N}_0}{n-ik+\mathfrak{N}_0}=\rho e^{i\phi}. \tag{3.10}$$

Then $\ln\rho(\omega)$ and $\phi(\omega)$ are the real and imaginary parts of the function $\ln r_N(\omega)$. If ω is taken to be a complex variable we can assert that this function is analytic everywhere in the upper half-plane [where the imaginary part of ω corresponds to damping of the wave (2.2)]. Then there must exist a set of Hilbert transforms[55] between $\ln\rho(\omega)$ and $\phi(\omega)$. Since a change in the sign of ω corresponds to time reversal, and hence to a change in the sign of the phase ϕ but not of the modulus ρ, these transforms reduce to

$$\begin{aligned}\ln\rho(\omega)&=\frac{2}{\pi}\int_0^\infty\frac{\omega'\phi(\omega')-\omega\phi(\omega)}{\omega'^2-\omega^2}d\omega',\\ \phi(\omega)&=\frac{2\omega}{\pi}\int_0^\infty\frac{\ln\rho(\omega')-\ln\rho(\omega)}{\omega'^2-\omega^2}d\omega'.\end{aligned} \tag{3.11}$$

These are one set of Kramers-Kronig dispersion relations,[56] first applied to reflectivity studies by Robinson.[57] The second of the two Eqs. (3.11) should enable us, from measurements of $\rho=R_N^{1/2}$, to calculate ϕ and hence, using Eq. (3.10), n and k.

In theory, this method is exact if $\rho(\omega)$ is known over the entire finite frequency range. In practice, since $R_N(\omega)$ can be measured over only a finite and usually quite small range, $\phi(\omega)$ is determined to an accuracy which depends on the extrapolation of $\rho(\omega)$ to zero and infinite frequencies. In liquid mercury, whose reflectivity has been measured at normal incidence from 30 μ (this work) to 20 eV,[32] this accuracy ought to be considerably greater than in most metals. Nevertheless, Wilson and Rice[32] have concluded that the insensitivity of R_N near the Hagen-Rubens region renders Kramers-

[55] See, e.g., P. M. Morse and H. Feshbach, *Methods of Theoretical Physics* (McGraw-Hill Book Co., New York, 1953), Vol. I, pp. 370 ff.

[56] Another set is derived somewhat more carefully by T. D. Landau and E. M. Lifschitz, *Electrodynamics of Continuous Media* (Addison-Wesley Publishing Co., Inc., Reading, Mass., 1960), pp. 256 ff.

[57] T. S. Robinson, Proc. Phys. Soc. (London) **B65**, 910 (1952).

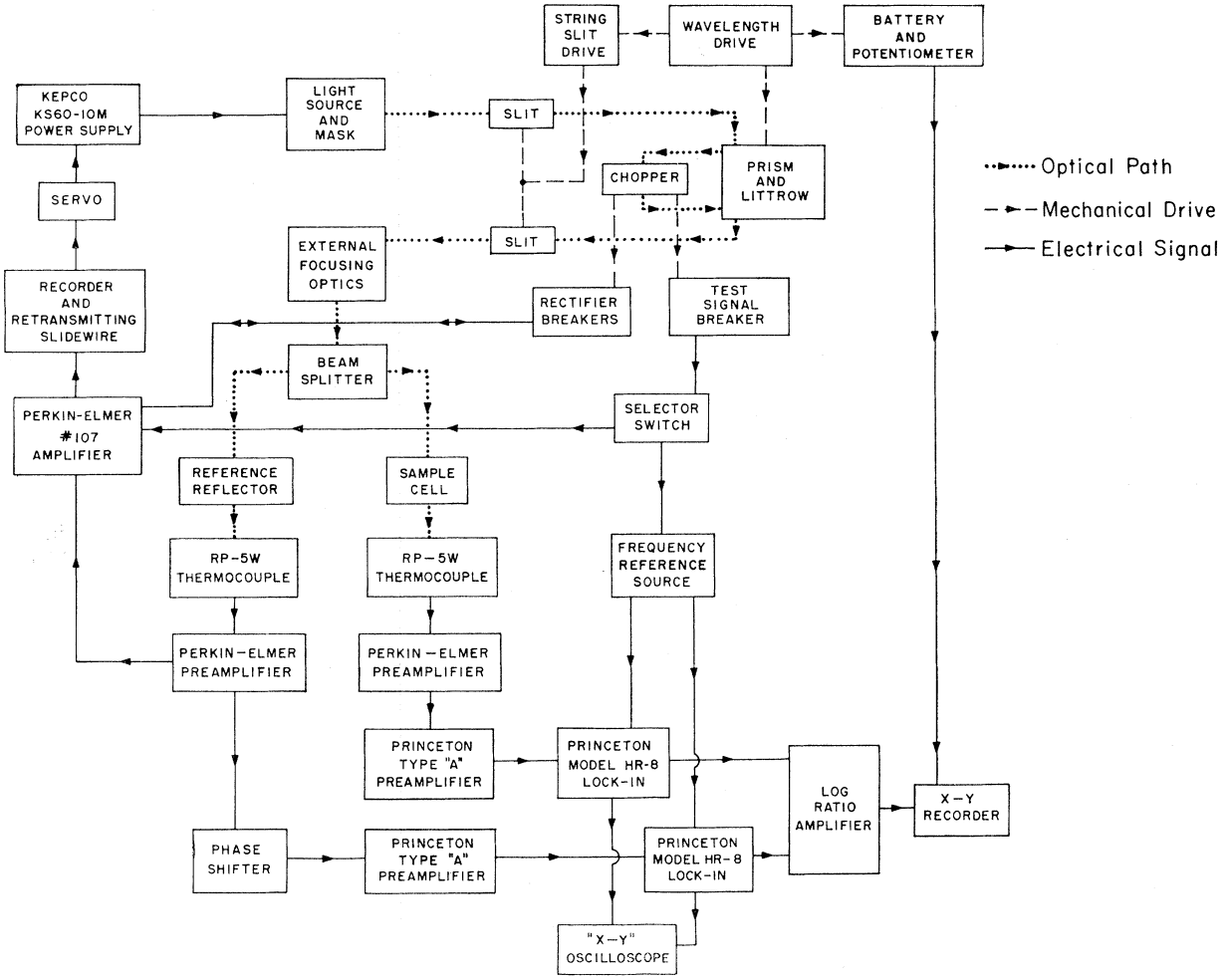

FIG. 3. Block diagram of the double-beam infrared reflection spectrometer.

Kronig analyses inadequate for absolute determinations of the optical constants of metals in the infrared.

With some experimental care, however, an alternative approach is available. We note that R_N in Eq. (3.5) is a function not only of n and k, but also of the index of refraction $\mathfrak{N}_0$ of the contact medium. It follows that pairs of contact media of known $\mathfrak{N}_0$ should furnish us with the simultaneous equations we require for the determination of n and k. Such media are readily available in the form of optical quality dielectric windows, and so we should be able to determine n and k exactly by measuring R_N for a series of sample-window interfaces.

Other considerations being equal, the success of this procedure will depend on two factors—the accuracy to which we know $\mathfrak{N}_0$ and the quality of our sample-window interface. In general, we know the real part n_0 of $\mathfrak{N}_0$ for most common window materials to at least five significant figures from the literature, and we can determine the imaginary part k_0 by performing transmission measurements. Meanwhile, the prospects for a good interface between a liquid sample and a window are greatly improved by letting the window form the bottom of the sample cell. In the bottom window geometry the weight of the liquid itself assures reasonably good contact even if the window is not wetted. Moreover, since oxide layers and most other common surface contaminants can be expected to float to the top, we can anticipate that with careful cell-filling techniques the contamination of the surface will be no worse than a thin film of gas adsorbed on the window surface. If r_1 and r_2 are the normal-incidence amplitude reflection coefficients of the window-gas and gas-sample interfaces, respectively, we find by summing the amplitudes of the infinite series of internal reflections that the total amplitude reflection coefficient for such a film of thickness d is given at normal incidence by[58]

$$r_{N\,\text{film}}=\frac{r_1+r_2e^{-4\pi id/\lambda}}{1+r_1r_2e^{-4\pi id/\lambda}}. \tag{3.12}$$

[58] O. S. Heavens, *Optical Properties of Thin Solid Films* (Butterworths Scientific Publication, Ltd., London, 1955), pp. 55 ff.

The difference between the R_N obtained using this equation and that given by (3.5) diminishes with increasing wavelength. At 5461 Å, close to the short-wavelength limit of the measurements performed in this work, a film of air 10 Å thick affects the reflectivity of a liquid mercury-lithium fluoride interface by about 0.13%. Even if the film expands to the improbable thickness of 100 Å, the effect remains less than 0.5%. At a wavelength of 2 μ the effect of a 10 Å film is completely negligible even for a window with index of refraction as high as that of KRS-5. We do not expect, then, that any of our results will be appreciably influenced by contamination of our surfaces, and this conclusion, as we shall see, is reinforced by our experiments on liquid mercury. We note in passing the contrast between this happy situation and the state of affairs in ellipsometric work, where the effect of films such as those we have just considered would be disastrous.[11,34b,35]

B. Description of the Apparatus

Our spectrometer rests on a massive optical bench whose base is fashioned from three limestone slabs, 3 ft square and 4 in. thick, set on edge and bolted together in an H configuration. The slabs were supplied by the South Chicago Stone Co. The top of the bench is a 1-in.-thick piece of aluminum, 4 ft square, obtained from the Central Steel and Wire Co., Chicago. It is flat to within 0.005 in.

The instrument itself is represented in the block diagram of Fig. 3. At its heart is a modified Perkin-Elmer Model 112U double-pass prism spectrometer, converted from a grating instrument by means of a convenient conversion kit purchased from the Perkin-Elmer Corp., Norwalk, Conn. To span the wavelength range of interest in the mercury studies we employed three physically interchangeable prisms, made, respectively, of calcium fluoride (<0.5–$7.0\,\mu$), sodium chloride (5.5–14.0 μ), and cesium bromide (8.5–$>30.0\,\mu$).

The source optics of the Model 112U include a mirror (not shown in Fig. 3) which can be rotated to intercept light from any of three permanently mounted sources. We chose a mercury arc for use in wavelength calibration and monochromator alignment, a high-intensity tungsten ribbon lamp (General Electric #9AT-8 1/2) for use in the visible and near infrared (<0.5–$3.5\,\mu$), and a Globar for use in the far infrared (1.5–$>30.0\,\mu$). The last two were operated by means of a Kepco KS 60-10M dc power supply, capable of powering either light source with a voltage or current regulation of better than 0.01%. This instrument presents the additional advantage of being programmable, a feature whose importance to us will shortly become evident.

The "light-source" block in Fig. 3 represents the appropriate source itself, the intercept mirror mentioned above, and a spherical mirror which focuses the intercepted light onto the entrance slit of the monochromator. Beyond the slit the diverging beam is collimated by an off-axis parabolic mirror, dispersed by the prism, and reflected back through the prism onto the off-axis paraboloid by a Littrow mirror. Refocused by the paraboloid, the beam is chopped at 13 cps, displaced slightly and passed through the entire paraboloid-prism-Littrow system a second time before being focused onto the monochromator exit slit. The wavelength of the light falling on this slit is determined by the angle of rotation of the Littrow mirror, which is in turn controlled mechanically by a graduated drum mounted on the side of the monochromator housing. This drum may be either set at a given wavelength by hand, or else rotated through a continuous scan by an electrically powdered drive mechanism.

The double-pass system functions effectively as a double monochromator, with two distinct advantages. First, it practically eliminates scattered light: Light scattered into the beam in the first pass is dispersed in the second, while light scattered into the beam in the second pass and beyond is not chopped, and will not be detected by our ac electronics. Second, it provides satisfactory resolution at much wider slit widths than does a single-pass instrument, so that light intensity and hence signal-to-noise ratio are augmented.

The slit width itself (identical for the entrance and exit slits) is controlled mechanically by a drum similar to the wavelength drum, and mounted near it on the monochromator housing. The two drums may be connected by means of a string wound on spiral pulleys attached to each. As the wavelength drum rotates over a scan toward longer wavelengths, this "string slit drive" continuously widens the slits. The spiral on the wavelength drum is a projection of the dispersion curve of a sodium chloride prism. With this prism in place, then, the string drive functions as a crude servomechanism to maintain a constant spectral slit width and, when the globar source is used, a relatively constant light intensity. In this way we can scan continuously and with constant resolution from the globar intensity peak to the long-wavelength limit of prism utility, without having to increase the gain of our electronics to the detriment of our signal-to-noise ratio. We have found that this device is quite effective when used in conjunction with either the sodium chloride or the calcium fluoride prism, but that it is less useful with the cesium bromide prism, since the CsBr dispersion curve is considerably steeper. The string drive could not be employed at all when the tungsten source was in operation, because most of the interesting wavelength region is on the high-energy side of the tungsten intensity peak, so that the intensity rises sharply, instead of falling, with increasing wavelength. On the other hand, the relatively short time constant characteristic of the tungsten filament enabled us to control the lamp intensity itself with an electronic servomechanism[59] acting upon the programmable Kepco power supply.

[59] The design and circuitry of this device are presented in detail by A. Bloch, Ph.D. thesis, University of Chicago (unpublished).

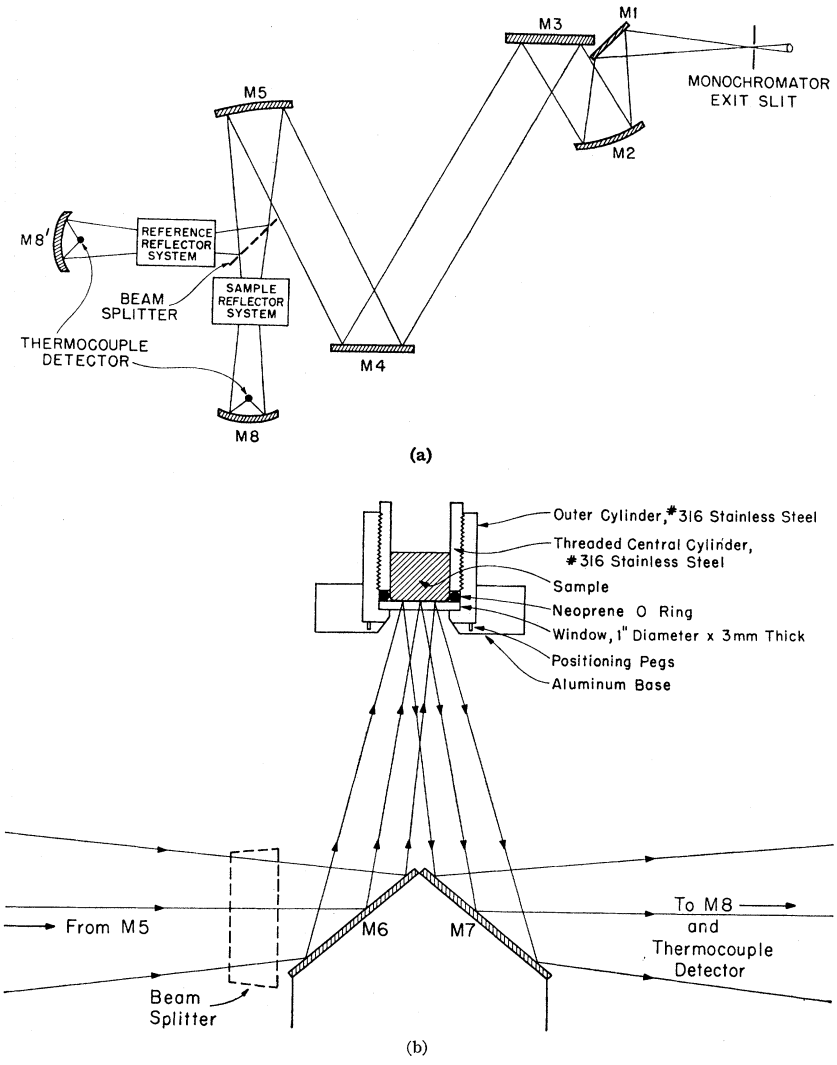

FIG. 4. (a) Sketch of optical path external to monochromator, top view (not to scale). In the reference and sample reflector systems, the beam is directed upward, out of the plane of the paper [cf. Fig. 4(b)]. (b) Sketch of optical path in the vicinity of sample reflector system, side view (not to scale). The reference reflector system is identical, but placed in the beam reflected by the beam splitter, out of the plane of the paper [cf. Fig. 4(a)].

The diverging monochromatic light beam which emerges from the monochromator exit slit enters an external optical system which is indicated by an appropriate block in Fig. 3 and sketched in detail in Fig. 4. To maintain light intensity even in regions of atmospheric absorption (and to prevent oxidation of the high-temperature cell), both the Model 112U and these external optics are enclosed in a gas-tight box which can be continuously flushed with argon or nitrogen.

Figure 4(a) shows the beam intercepted at 45° incidence by a flat mirror $M1$,[60] and reflected onto a 21° off-axis parabolic mirror $M2$. The paraboloid is placed one focal length (26.7 cm) from the exit slit, so that the beam it reflects onto the flat mirror $M3$ is collimated. The mirrors $M1$–$M3$ are all mounted on an aluminum platform bolted to the monochromator housing, and serve as a general-purpose parallel-beam unit which converts the monochromator output into a form which may be adapted to virtually any optical system we may wish to design. The quality of the collimation is such that the cross-sectional beam dimensions change by less than 20% over the length of a room.

The remainder of the external optical system is mounted on a versatile frame of small-channel (13/16×13/32 in.) Unistrut. This arrangement allows new components to be added and old ones to be moved and adjusted conveniently without need for any major disruption such as drilling new holes. The first component on the frame is the flat mirror $M4$, which returns the beam to the paraboloid $M5$, a duplicate of $M2$ and

[60] This and all other mirrors used in the system were front-surface aluminum reflectors sold by the Perkin-Elmer Corp. as components for various of their commercial spectrometers. J. B. McDaniel, Appl. Opt. 3, 152 (1964) has described a procedure for cleaning dust, fingerprints, etc., from these mirrors using collodion solution. We have obtained superb results with this technique, which does not require removing the mirrors from their mounts or disturbing their alignment in any way.

of the monochromator paraboloid. The converging beam reflected from $M5$ is now intercepted by the beam splitter. Two such devices were used interchangeably: a single crystal of calcium fluoride, half-silvered in a polka-dot pattern and effective out to its 9-μ transmission cutoff, and a slab of KRS-5 (thallium bromide-iodide). The index of reflection of KRS-5 is so high ($\sim$2.4) that its reflection coefficient for light of arbitrary polarization at 45° incidence is comparatively large throughout the far infrared, but it absorbs strongly at short wavelengths, where we therefore employ the calcium fluoride splitter.

The reflected and transmitted beams now strike respective mirrors which reflect them upward, out of the plane of Fig. 4(a). Figure 4(b) shows a side view of the path of the transmitted beam; the configuration for the reflected beam is identical. Mirrors $M6$ and $M7$ are set on an aluminum block at angles of 40° to the horizontal. The angle of incidence upon the front surface of the sample cell window, or upon the standard reflector, is thus 10°; the angle of incidence upon the sample-window interface itself will be still less, owing to refraction at the front window surface. We defer for the moment a discussion of the problem of reflection from this surface.

The sample cell (or the standard reflector) is supported by the Unistrut frame at a height so chosen that the beam achieves its focus at the sample-window interface (or the reflecting surface of the standard). As designed for liquid mercury, the cell itself, shown in Fig. 4(b), is a simple cup consisting of two concentric stainless steel (Type 316) cylinders. The window, 1 in. in diam and 3 mm thick, forms the bottom of the cup and rests on a lip at the base of the outer cylinder. The inner cylinder is screwed into the outer one and seals the window by means of a neoprene O ring. The cell is positioned by brass pegs in a well cut in an aluminum block, which, in turn, is bolted to the Unistrut frame and serves as a base. For filling or cleaning the cell can simply be lifted out of the well.

Finally, the diverging beam reflected by the sample or standard is directed by $M7$ to the spherical mirror $M8$ [Fig. 4(a)], which focuses it, with a six-to-one reduction in size, onto the thermocouple detector target. The path of the second beam, via the spherical mirror $M8'$, is analogous. Both detectors are Reeder Model RP-5W thermocouples with cesium bromide windows; we found these to be more sensitive than their Perkin-Elmer counterparts by a wavelength-dependent factor of 5–10.

The radiation falling on the detectors will be the sum of several different components: scattered light, background radiation (including room lights and thermal emission from various parts of the optical system), unchopped light from the first pass through the monochromator, and the 13-cps chopped beam from the second pass. Then the electrical output of each thermocouple must consist, in addition to Johnson noise generated by its 10-Ω impedance, of a direct current corresponding to the first three radiation components, transients from instantaneous variations in the first and second, the 13-cps ac signal from the fourth, and 60 cycle and rf pickup. Our problem now is to amplify the 13-cps signals, which in most circumstances are of the order of microvolts, while rejecting the others.

We can immediately eliminate the dc components by transformer-coupling each detector to its own Perkin-Elmer thermocouple preamplifier. These carefully shielded devices utilize a high-gain pentode to amplify the ac components, transients, and noise at a gain of about 9000, while generating remarkably little internal noise of their own. When we tried to replace these preamplifiers by Princeton Model AM-1 step-up input transformers, we found to our surprise that our signal-to-noise ratio suffered by a factor of 5.

The Perkin-Elmer thermocouple preamplifier was designed to operate as an integral part of the Perkin-Elmer Model 107 Amplifier, a narrow-band device whose last stage is a rectifier synchronized with circuit breakers mounted on the base of the 13-cps chopper. In the original single-beam instrument the RC output network of the preamplifier leads to the first stage of the 107 amplifier, and eventually to a Leeds and Northrup Type G recorder which registers I or I' of Eq. (3.8). We have left these connections intact in order to be able to use this recorder to register standard emission and absorption spectra for use in wavelength calibrations, to monitor separately the characteristics of one beam while measuring the double-beam ratio, and, by means of a retransmitting slidewire, to activate the servomechanism for the tungsten lamp.

Prior to the first stage of the 107, however, we have tapped the signal from the preamplifier output network and fed it into a Princeton Model HR-8 lock-in amplifier with a type A (high input impedance) preamplifier. For double-beam operation we have built into the Model 107 a duplicate RC thermocouple preamplifier output newwork which leads to a second Model HR-8. Both HR-8's are tuned to a 13-cps square wave produced by applying a battery voltage to a rotating microswitch mounted on the shaft of the light chopper. This switch originally served as a circuit breaker for a 13-cps electrical signal which could be passed through the output resistor of the thermocouple to test the Perkin-Elmer electronics independently of the optics. We have installed in our system a selector switch which may be used to restore this circuit at the expense of our HR-8 frequency reference source.

Tuned to the chopper in this way, the HR-8's reject any ac components, including 60 cycle and rf pickup, which are detectably different from the chopper frequency, and damp the effects of transients. With a frequency rolloff setting of 12 dB/octave and a Q of 10, the internal noise generated by the lock-ins and their preamplifiers is sufficiently low for our over-all noise

level still to be determined by the Johnson noise of the 10-Ω thermocouples themselves.

The advantages of this high selectivity, however, will be washed out by beats between the two HR-8's unless special care is taken in tuning them together. This double tuning is considerably expedited by monitoring on a Hewlett-Packard 130B oscilloscope the Lissajous figures formed by the outputs of corresponding channels of the two lock-ins. If the two signals are alike not only in frequency, but also in phase, the tuning may be accomplished with considerable accuracy and sensitivity by requiring that the final Lissajous figures be straight lines. However, the phases of the Perkin-Elmer preamplifier outputs are generally different because of the different response times of the two thermocouples, and because of the difficulty in duplicating exactly an *RC* output network composed of 1 and 5% resistors, and 5 and 10% capacitors. This situation is corrected by inserting into one channel a continuously variable *RC*-active phase shift network,[61] which may be adjusted to make the outputs of the HR-8 signal-tuned amplifiers equal in phase.

The filtered dc outputs of the lock-ins are fed through resistances into respective Philbrick solid-state operational amplifiers with matched logarithmic transconductors in their negative feedback loops; the output of each of these devices[59,62] is then proportional to the logarithm of the current through the resistance, and hence of the HR-8 output voltage. Finally, a third operational amplifier[63] measures the difference between the two signals. This quantity is proportional to the logarithm of the ratio I'/I (or I''/I), and is plotted on one axis of a Moseley X-Y recorder. The other axis registers wavelength by means of a battery voltage across a potentiometer fastened to the rotating wavelength drum on the monochromator.

C. Experimental Procedure and Results

As we have pointed out during the course of our description of the apparatus, the limits on the sensitivity of our method are no worse than those imposed by the Johnson noise of the 10-Ω thermocouple detectors. With a 3-sec time constant on the HR-8's and a flat aluminum mirror as the standard reflector R', this noise level is such that our signal-to-noise ratio typically approaches 10^4.

The limits on our accuracy, however, are determined by the accuracy with which we know the optical properties of our window and of the reflector R''. It is difficult to find a metal reflector suitable for use as R'', partly because of the sensitivity of the reflectance of such materials to this condition of the surface and to crystal strains, and partly because the normal reflectivities of most metals are not known to an accuracy any better than that to which we know the reflectance of mercury to begin with. We can avoid this problem, and consolidate our two uncertainties into one, by using for R'' a windowed empty cell.

This procedure leads to some loss in signal-to-noise ratio owing to the comparatively low reflectivity of dielectric windows, but the gain in accuracy is well worth the sacrifice. As we have stated earlier, we generally know the real part n_0 of the window index of refraction to at least five significant figures, and can determine the imaginary part k_0 from transmission measurements.

The energy reflection coefficient R_N for a metal-window interface is given by Eq. (3.5). For a window-atmosphere interface the corresponding expression is

$$R_0=\frac{(n_0-1)^2+k_0^2}{(n_0+1)^2+k_0^2}. \tag{3.13}$$

Then by summing the infinite series of coefficients of internal reflections in a flat window at normal incidence, we obtain for the total reflectivity of the window of a cell filled with mercury the expression

$$R'=R_0+(1-R_0)^2R_Nt^2/(1-R_0R_Nt^2), \tag{3.14}$$

where t is the bulk transmittance of the window. The accuracy of this equation in real situations is assured by its rapid convergence: after only three internal reflections the sum for mercury: KRS-5 is negligibly different from (3.14). [This expression could also have been obtained by averaging Eq. (3.12) over all phases, on the assumption that in a thick window surface irregularities are of the order of wavelengths of light.]

For an empty window, (3.14) reduces to

$$R''=R_0\left(\frac{1-2R_0t^2+t^2}{1-R_0^2t^2}\right). \tag{3.15}$$

The transmission of such a window is

$$T=(1-R_0)^2t/(1-R_0^2t^2). \tag{3.16}$$

It is easy to verify that for a dielectric in the infrared region of the spectrum, the transmittance t, as determined by Beer's law and the absorption coefficient $2n_0k_0\omega/c$, will be quite small before k_0 is large enough to affect R_0. Then if we know n_0, we know R_0 from (3.13), and can calculate t directly from measurements of T. Using this value of t, we can obtain R_N directly from our measurements of the ratio R'/R''.

Four window materials were used in the liquid mercury studies: lithium fluoride,[64] sodium chloride,[65]

[61] For a good general account of such devices, see *Handbook of Operational Amplifier Active RC Networks* [Burr-Brown Research Corp., Tuscon, Ariz., 1966].

[62] The advantages of this method of measuring the ratio were first pointed out to the authors by Dr. David Beaglehole.

[63] The principles of operation of such amplifiers are lucidly presented in *Handbook of Operational Amplifier Applications* [Burr-Brown Research Corp., Tuscon, Ariz., 1963].

[64] Values for n_0 for this substance were obtained graphically from the data of J. Durie, J. Opt. Soc. Am. **40**, 878 (1950); also, Ref. 53, p. 59.

[65] n_0 from W. W. Coblentz, J. Opt. Soc. Am. **4**, 443 (1920).

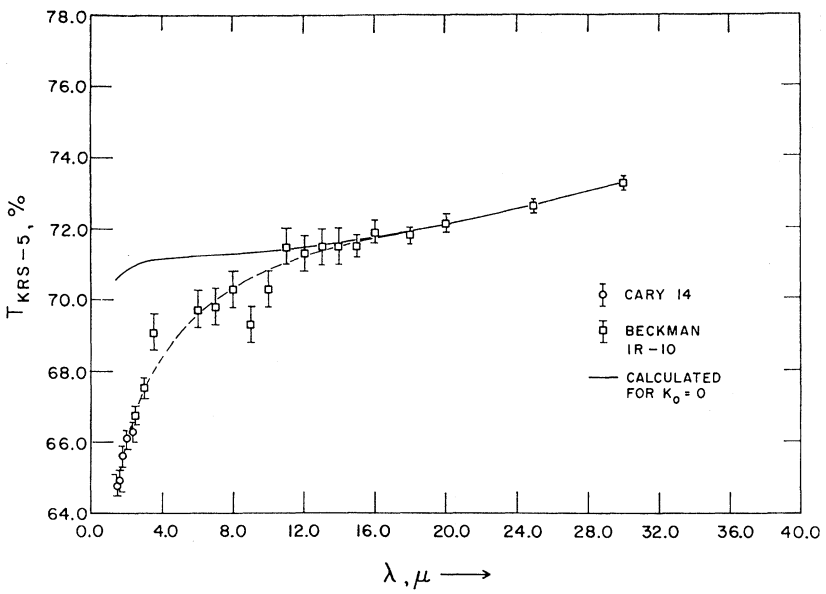

FIG. 5. Transmission of KRS-5 window, 3 mm thick, used to obtain data of Fig. 6.

cesium bromide,[66] and KRS-5.[67] Of these, the second and third rapidly adsorbed moisture, which rendered the results in water absorption regions erratic and unreasonable. This same phenomenon apparently caused diffraction effects at the surfaces of these two windows in the short-wavelength region, with similar consequences. Otherwise, the measured transmission of all windows, as determined using Cary 14 and Beckmann IR-10 spectrometers, agreed quantitatively with results calculated for $t=1$, except for KRS-5. The measured transmission of this material, compared with the value calculated for zero absorption, is plotted in Fig. 5.

The liquid mercury data themselves were obtained in one of two ways. Where the signal-to-noise ratio was high enough to permit a 3-sec time constant to be used in the HR-8 filters, each new mercury surface was scanned continuously over the appropriate spectral region. In the far infrared, where source intensity was too low to obtain a good signal-to-noise ratio using a 3-sec time constant, a 30- or 100-sec filter was used and the measurements taken point by point. At any wavelength, several minutes were therefore required for the system to reach equilibrium; to minimize the possibility of electronic drift over these time periods the sample and empty window were measured consecutively at each wavelength. Each wavelength point in our measurements, then, corresponds to an average of two or three new surfaces, different from those at any other point. The relatively small scatter in our results (usually $\pm 0.2\%$; in the worst cases $\pm 0.5\%$) suggests that our surfaces were, as predicted, clean enough for purposes of normal reflectivity measurements: If they were dirty, they were dirty to an astonishing degree of reproducibility.

Figure 6 is a plot of our values of R_N for a mercury: KRS-5 interface, calculated from our data for $\ln R'/R''$ using formulas (3.14) and (3.15) and the data of Fig. 5. The Drude curve is also shown; we take the general agreement to be excellent. The exceptions at short wavelengths (to be compared with the data of Hodgson,[30] recalculated to normal incidence and a KRS-5 interface) are not reproduced using other windows, and seem to be a product of the uncertainties in the values of t in this region as measured in Fig. 5. We have indicated separately the points obtained using different prisms in the monochromator. This separation of the data is intended to recognize the small variations in focus that often accompanied changes of prisms. Such a change apparently occurred between the NaCl and CsBr prisms in the region 10–15 μ, but since the relative positions of the two sets of points are reversed for mercury: cesium bromide interfaces (Fig. 7), we are inclined not to take seriously the slight deviations from Drude values found here with the NaCl prism.

Figure 7 shows some of the data obtained for mercury: sodium chloride and mercury: cesium bromide interfaces. Because of the water adsorption problem we did not pursue these measurements as extensively as we did those involving the other two window materials. The larger scatter of the data for cesium bromide: Hg interfaces at long wavelengths is a consequence of the low reflectivity of the empty window (compared with KRS-5) in this region.

In Fig. 8 we present our results, using the tungsten lamp and servomechanism, for mercury: lithium-fluoride interfaces over a wavelength region similar to that covered by Faber and Smith[34] and by Hodgson.[30] Their

[66] n_0 from W. S. Rodney and R. J. Spindler, J. Res. Nat. Bur. Std. **51**, 123 (1953).
[67] n_0 from *Synthetic Optical Crystals* (Harshaw Chemical Co., Cleveland, 1955), pp. 23–24.

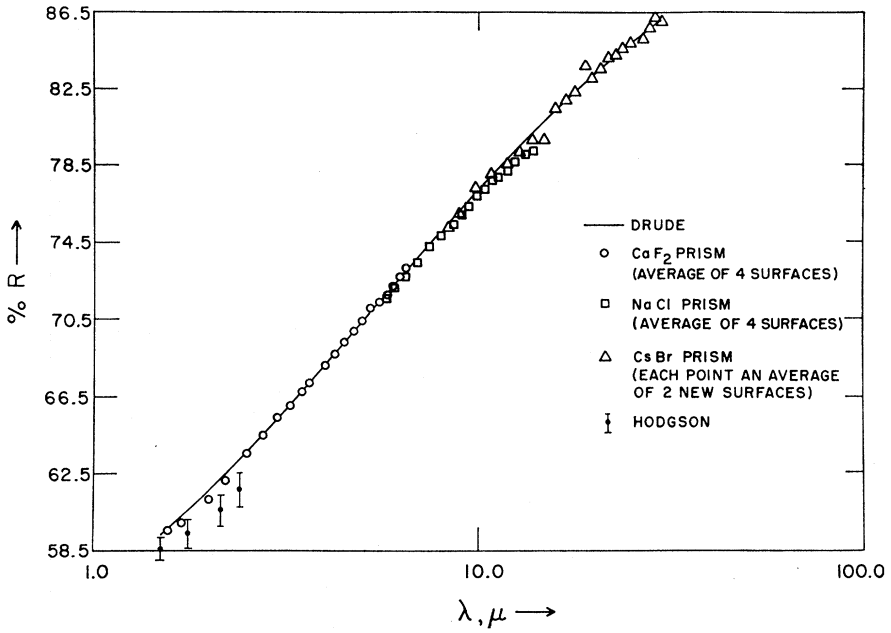

FIG. 6. Reflectivity of Hg: KRS-5 interface, 1.50–30.0μ. Separate data are recorded for each prism used to allow for possible focusing errors, as explained in the text. The results of Hodgson (Ref. 30) recalculated to normal incidence, are also shown, and both sets of data are to be compared with the solid curve, calculated from simple Drude theory.

recalculated data are also presented. These are well outside the limits of our experimental error, as our data and the Drude curve are outside theirs.

From the agreement between our data and the Drude curves it is obvious that there is no point to pursuing our original plan of using different values of n_0 and R_N at given wavelengths to obtain optical constants. We regard our data as substantial confirmation of the conclusions of Schulz,[28] Wilson and Rice,[32] and Boiani and Rice[38] that they affect its absolute reflectivity, the apparent optical constants of liquid mercury are not appreciably different from their classical Drude values.

IV. DISCUSSION

The results of Sec. III have confirmed that there is a genuine and measurable difference between the ellipsometric properties of liquid mercury and its optical properties as determined by studies of its absolute reflectivity. We know of no way to explain this discrepancy except by invoking the surface effects discussed in Sec. II.

There are, of course, two points of view that may now be adopted. First, we might say that the available data are insufficient to determine the properties of both the

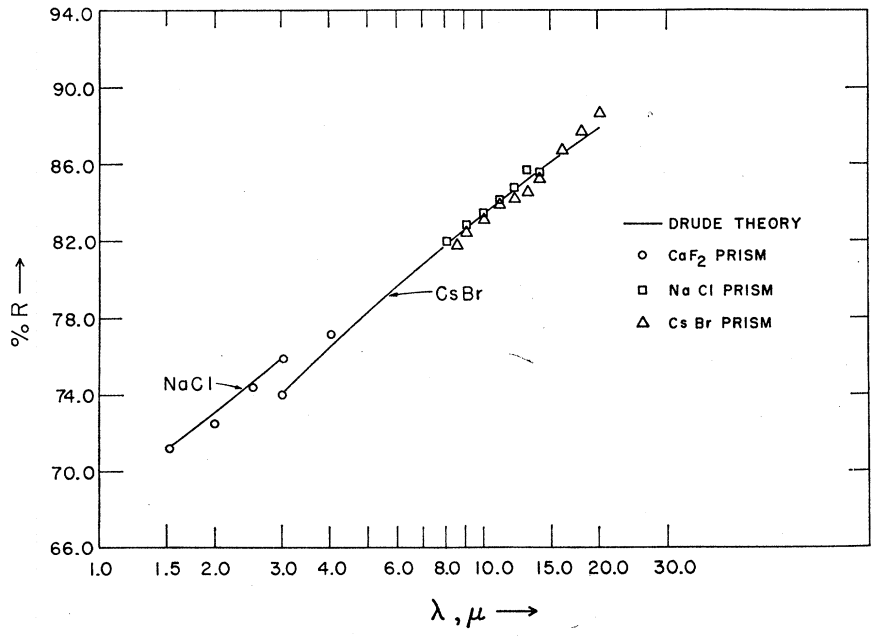

FIG. 7. Reflectivity of Hg: NaCl and Hg:CsBr interfaces, 1.50–20.0μ. Again, the solid curves represent the predictions of simple Drude theory.

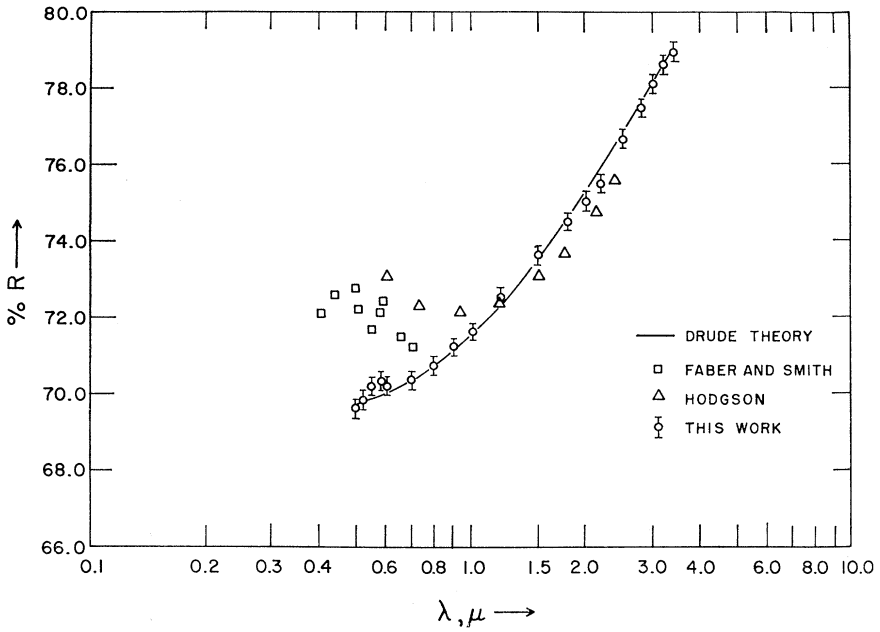

FIG. 8. Reflectivity of Hg: LiF interface, 0.495–3.40 μ. The results of Faber and Smith (Ref. 34) and of Hodgson (Ref. 30), recalculated to normal incidence, are displayed for comparison. We do not show the experimental uncertainty in their data, which amounts to as much as $\pm 1.8\%$ in the reflectivity (cf. Fig. 6). As usual, the Drude theory is represented by the solid curve.

surface and bulk material, and hence we cannot interpret the measurements. Alternatively, we could accept the reality of the surface effect and see whether any "reasonable" model of the surface will permit representation of all of the observations and their interpretation in terms of optical constants for both surface and bulk liquid. It is the second alternative which we adopt in this Discussion.

Whether we can convert this point of view into any sort of a useful quantitative argument is another question entirely. The fact remains, when all is said and done, that we know next to nothing about the real nature of the surface of a liquid metal, and that even our guesses are at this point distinctly uneducated. Nevertheless, we are not without a few tenuous guidelines, and we shall try to make use of these as best we can.

If we are to understand the optical properties in these terms, we need first to be able to offer some description of the profile followed by the conductivity as we move across the transition zone. At the outset we can reasonably require that this profile and its space derivatives be everywhere continuous and finite, but our only other information about its form is that it must be anchored at one extreme by the bulk conductivity (which we shall assume to obey the Drude formula), and at the other by the conductivity of the contact medium (which we shall take to be the vacuum).[68]

It may seem natural at first to argue, on the assumption that the free electron density should follow the ion density, that the conductivity should vary monotonically between the bulk and vacuum limits. A little reflection, however, shows us that this is not necessarily the case. In the first place, even if the ion density transition is a discontinuous step function in the variable z, the change in electron concentration need not follow suit. Ewald and Juretschke[69] have pointed out that if the surface of a free-electron metal is regarded as an infinite potential barrier the electronic charge density in the vicinity of that surface must rise continuously from zero to a maximum, located approximately one interionic distance from the barrier, before being damped gradually to its bulk value. They are able to account for some of the features of the surface energetics of liquid metals by recognizing that this maximum corresponds to a dip in the average exchange potential near the surface. For our purposes, of course, it may also correspond to a maximum in the conductivity.

This phenomenon may persist to some extent in the presence of a finite barrier and an ion density transition zone of nonzero width. Moreover, we shall now argue that in certain systems it may be enhanced by the structural influences upon the conductivity which must occur in such a zone.

[68] Our choice of the vacuum instead of a dielectric window is simply for convenience in comparing our results with ellipsometric data, most of which were obtained with free surfaces. We speculate that if a window were introduced, its primary physical effect, provided it were not wet by the mercury, would be to eliminate the low-density (vapor) tail of our profile. This should have a negligible influence on absolute reflectivity measurements, as the agreement of our results and those of Schulz (Ref. 28) with those of Wilson and Rice (Ref. 32) and of Boiani and Rice (Ref. 38) attests. Ellipsometric measurements would be far more sensitive to such a perturbation, and Faber and Smith (Ref. 34) do report results for mercury-quartz interfaces that are significantly different from those they obtained for free mercury surfaces.

[69] P. P. Ewald and H. Juretschke, in *Structure and Properties of Solid Surfaces*, edited by R. Gomer and C. S. Smith (University of Chicago Press, Chicago, 1953), pp. 82 ff.

We consider first the effect of the surface tension. In the early theories of this quantity,[70] it was fashionable to speak in terms of "partial bonds": A surface metal atom, for example, having only half as many nearest neighbors as its counterparts in the bulk, shares twice as many "partial metallic bonds" with each near neighbor; hence there should be a smaller separation and the familiar tendency toward contraction of the surface.

Kirkwood and Buff[71] have offered a mechanical definition which carries much the same force. They define the surface tension as the excess stress per unit width, relative to a Gibbs[72] dividing surface, acting across a strip placed normal to that surface. They develop a statistical mechanical theory of the surface tension according to this definition, and find that one result of this stress is that the excess surface density of matter per unit area, again relative to the Gibbs boundary, is positive. This confirms an earlier conclusion of Tolman,[73] based on a quasithermodynamic treatment of the surface tension.

Now if we accept the recent conclusion of Eyring and co-workers[74] that in liquid mercury several atomic layers must contribute to the surface tension, we may surmise that this compression effect must extend over those layers, and that it may even produce a layer whose density is higher than the bulk value. Systems exhibiting similar effects are not unknown. Long ago Lennard-Jones and Dent[75] put forth the claim that the interplanar spacing in alkali halide crystals is smaller between the outermost planes parallel to the surface than between planes in the bulk. Likewise, when the surface atoms of a thin metal wire or silica fiber are forced to share some of their "partial bonds" with an adsorbant, the strand is found to lengthen by an amount which increases with the strength of the adsorption.[76]

"Partial bonds" or no, it is clear that the surface tension is essentially a contracting force, and contraction, in a divalent metal, should tend to increase the overlap and enhance the conductivity. If it is really true, then, that this contraction can produce densities higher than those in the bulk, it is not implausible that in some liquid metals the conductivity actually does pass through a maximum as we traverse the surface zone.[77]

In fact, in the case of liquid mercury there is some indication that the maximum may be rather dramatic. As we mentioned in Sec. II, Mott[12] has reinterpreted the properties of this metal in terms of the liquid structure as recently determined by Rivlin *et al.*[78] These workers found that the main peak in the structure factor, $a(K)$, is displaced somewhat to the left of its position in other metals, and that a shoulder appears on the right. The two maxima correspond closely to the nearest-neighbor distances in the two known allotropes of solid mercury, the rhombohedral α-Hg,[79] and the low-temperature, high-pressure tetragonal β-Hg.[80] Both allotropes are distortions of the fcc structure, and are attributed by Heine and Weaire[81] to the proximity of the zero, K_0, of the pseudopotential, $v(K)$, to the main structural weight, $W(\mathbf{g})$, of the reciprocal lattice vectors, $\mathbf{g}$, in the close-packed structure. Heine and Weaire represent the binding energy of the crystal as the sum of an electrostatic Ewald term[82] and a band-structure term which depends on the product $W(g)[\tilde{v}(g)]^2$. Any distortion which moves $W(g)$ away from K_0 rapidly enhances the contribution of the band-structure term, but only at the expense of the Ewald term. The balance is a delicate one, with the distortions favored by only 0.01 eV according to the figure quoted by Mott.[12] The measurements of Rivlin *et al.* seem to confirm the prediction of Heine and Weaire that this balance should persist in the liquid, and on that basis Mott is able to explain most of the abnormal properties of bulk liquid mercury.

This is no guarantee, however, that the balance will also persist in the presence of a surface tension, which should, if our interpretation is correct, act as a positive correction to the electrostatic term. The tendency toward close packing would then be enhanced in the surface zone and we should expect the relevant structure factor there to be less similar to the result of Rivlin *et al.* than to the calculated result of Ashcroft and Lekner.[83] Animalu,[84] taking no account of the work of Rivlin *et al.*, has used the Ashcroft-Lekner structure factor to calculate electrical properties for mercury according to Ziman's[13] theory. His result for the dc conductivity is higher than the measured bulk value by a factor of nearly 3.

Even if our density does increase to a close-packed value in a few atomic layers near the surface, it must quickly begin to decrease again to the vapor level. But the corresponding decrease in conductivity need not be so rapid. Mott[27] quotes an experimental value of

[70] See, e.g., H. H. Uhlig, in *Metal Interfaces* (American Society for Metals, Cleveland, 1952), pp. 312 ff.

[71] J. G. Kirkwood and T. P. Buff, J. Chem. Phys. **17**, 338 (1949).

[72] J. W. Gibbs, *Collected Works* (Longmans, Green & Co., New York, 1928), Vol. I, p. 219.

[73] R. C. Tolman, J. Chem. Phys. **17**, 118 (1948).

[74] W. C. Lu, M. S. Jhon, T. Ree, and H. Eyring, J. Chem. Phys. **46**, 1075 (1967).

[75] J. E. Lennard-Jones and B. M. Dent, Proc. Roy. Soc. (London) **A121**, 247 (1928).

[76] C. Benedicks, in Proceedings of the International Conference on Surface Reactions, Pittsburgh, 1948, p. 196 (unpublished).

[77] An interesting analogy is found in the case of optically polished solid specimens of the semimetal tellurium. The surfaces of such specimens consist of a conducting layer which disappears on etching; see P. W. Kreise, L. D. McGlauchlin, and R. B. McQuistan, *Elements of Infrared Technology* (John Wiley & Sons, Inc., New York, 1962), p. 151.

[78] V. G. Rivlin, R. M. Waghorne, and G. L. Williams, Phil. Mag. **13**, 1169 (1966).

[79] R. F. Mehl and C. S. Barrett, Trans. AIME **89**, 575 (1930).

[80] M. Atoji, J. E. Schirber, and C. A. Swenson, J. Chem. Phys. **31**, 1628 (1959).

[81] V. Heine and D. Weaire, Phys. Rev. **152**, 603 (1966).

[82] See, e.g., N. T. Mott and H. Jones, *The Theory of the Properties of Metals and Alloys* (Clarendon Press, Oxford, 1936), p. 142.

[83] N. W. Ashcroft and J. Lekner, Phys. Rev. **145**, 83 (1966).

$(\partial \ln\rho/\partial \ln V)$ for bulk mercury of $+8$; Animalu[84] calculates -2; and we expect that our surface value would lie somewhere in between. If so, the conductivity may change only slowly, or even increase slightly for a range, as the close-packed disordered lattice is expanded.

Finally, when the density becomes low enough, localized states begin to appear. Ewald and Juretschke[69] speculate that the contribution of such localized surface states may account for some of the discrepancy between calculated and measured values of the total surface energy in metals, and Stern[85] has suggested that they may account for the anomalous absorptions observed in alkali metals by Mayer and co-workers.

Our conjectural conductivity profile, then, increases from the bulk Drude value to a maximum, and then gradually decreases to the vapor level. As it decreases, the dispersion law for the conductivity changes from a Drude-like free-electron form to a Lorentzian, characteristic of the low-density hopping. It would be absurd, of course, to imagine that all this literally takes place over the space of the few interatomic distances to which our surface transition zone is confined. It is undoubtedly far more realistic to envision the surface conductivity as arising from a jumble of many processes, some displaying dispersion laws that are perhaps quite different from the simple formulas we are accustomed to dealing with in the bulk. The thrust of our discussion has simply been to propose that some of these processes may lead to conductivities higher than Drude values, and that some may be free-electron-like while others may involve energy barriers.

If the content of this section has so far been a rather cavalier exercise in guesswork, it has not been intended to lead to any firm conclusions, but rather to provide a framework for the calculation we are now about to undertake. Bearing in mind that they are always to be taken with a grain of salt, then, we should like to discover how well the above considerations can account for the observed optical behavior of liquid mercury.

We return to the inhomogeneous conductor problem of Sec. II and recognize that if our surface conductivity profile does pass through a maximum it might be closely approximated by the Epstein profile

$$\sigma(w)=\frac{-\sigma_b w}{1-w}-\frac{\sigma_s w}{(1-w)^2},\quad w\equiv -e^{z/\Delta}. \tag{4.1}$$

We identify the coefficient σ_b of the first term with the bulk conductivity of mercury, and assumes that it takes on the Drude values. For the moment we shall defer the treatment of the second term, which passes through an extremum.

We have already noted, in Sec. II, that Maxwell's equations cannot be solved analytically for this profile in the case of a TM wave at oblique incidence. Moreover, the analytic solutions for a TE wave lead to reflection coefficients which, as we have seen, are a product of gamma functions of complex arguments, not amenable to numerical evaluation. We can approximate the true solutions for both cases as closely as we like, however, by considering the inhomogeneous layer as a pile of homogeneous films of differential thickness, lying perpendicular to the z axis. The conductivity in the jth thin film is given by the value of the Epstein profile (4.1) at $z=z_j$, the plane of the film's low-z surface. The solutions of Maxwell's equations within each film are plane waves, and are subject to the usual boundary conditions at the (ideal) film surfaces. The advantage of such a stratified model over the continuous one is that not only can the results for both types of wave be easily calculated, but the model is more versatile: the dispersion law for the conductivity can be varied almost arbitrarily with z_j without raising any serious mathematical complications.[87]

In standard treatments of stratified media[88,89] it has become customary to introduce at this point the characteristic matrices of Abelès,[90] and to use them to calculate the optical properties. We find it conceptually somewhat more direct to turn instead to a simple extension of the equivalent matrices of Herpin,[91] from which those of Abelès may be derived.

We summarize this extension as follows. Let us consider a stack of L homogeneous thin films separating two semi-infinite, continuous, homogeneous media. Let one of these media be the vacuum, and the other our bulk liquid metal. We characterize the jth film, of thickness δ_j, by the complex dielectric constant $\epsilon_j(\omega)=1-4\pi i\sigma_j(\omega)/\omega=\mathfrak{N}_j^2(\omega)$, where $\mathfrak{N}_j(\omega)$ is the complex index of refraction. From Snell's law, the complex angle of refraction φ_j is related to the angle of incidence φ upon the first film by

$$\cos\varphi_j\equiv(1-\sin^2\varphi_j)^{1/2}$$
$$=\left(1-\frac{\epsilon_{j-1}}{\epsilon_j}\sin^2\varphi_{j-1}\right)^{1/2}$$
$$=\left(1-\frac{\epsilon_{j-2}}{\epsilon_j}\sin^2\varphi_{j-2}\right)^{1/2}=\cdots=\left(1-\frac{\sin^2\varphi}{\epsilon_j}\right)^{1/2}. \tag{4.2}$$

Then the plane-wave solutions in the jth film can be written for the tangential components of the TE wave in the form

$$E_y=ae^{-ip_jz}+be^{ip_jz},$$
$$H_x=-g_jae^{-ip_jz}+g_jbe^{ip_jz}, \tag{4.3a}$$

[84] A. O. E. Animalu, Advan. Phys. **16**, 605 (1967).
[85] E. A. Stern, in Proceedings of the Fourth International Materials Symposium, Berkeley, 1968 (unpublished).
[86] H. Mayer and B. Hietel, in Ref. 31, p. 47.
[87] R. Jacobsson, in *Progress in Optics*, edited by E. Wolf (North-Holland Publishing Co., Amsterdam, 1966), Vol. 5, pp. 266 ff.
[88] Reference 7.
[89] Reference 58, pp. 69 ff.
[90] F. Abelès, Ann. Phys. (Paris) **3**, 504 (1948); **5**, 596 (1950).
[91] A. Herpin, Compt. Rend. **225**, 182 (1947).

and of the TM wave in the form

$$E_x = ce^{-ip_j z} + de^{ip_j z},$$
$$H_y = h_j ce^{-ip_j z} - h_j de^{ip_j z}, \tag{4.3b}$$

where $p_j = (\omega/c)(\epsilon_j - \sin^2\varphi)^{1/2}$, $g_j = (\epsilon_j - \sin^2\varphi)^{1/2}$, and $h_j = \epsilon_j/(\epsilon_j - \sin^2\varphi)^{1/2}$; the functions a, b, c, and d are all of the form

$$a(x,\omega,t) = a_0 e^{i\omega(t - x\sin\varphi)}. \tag{4.3c}$$

Since the development from this point is of the same form for both cases, we shall treat only the TE wave in detail, and present the results for the TM wave at the end.

We consider first the sum and difference of the two equations (4.3a) and define

$$X \equiv -g_j E_y + H_x = -2g_j a e^{-ip_j z},$$
$$Y \equiv -g_j E_y - H_x = -2g_j b e^{+ip_j z}, \tag{4.4}$$

representing wave traveling in the positive- and negative-z directions, respectively. Then the column matrix

$$(A) \equiv \begin{pmatrix} E_y \\ H_x \end{pmatrix} \tag{4.5}$$

is related to the column matrix

$$(Z) \equiv \begin{pmatrix} X \\ Y \end{pmatrix} \tag{4.6}$$

by

$$(Z) = (T_j)(A), \quad (A) = (T_j)^{-1}(Z), \tag{4.7}$$

where

$$(T_j) = \begin{pmatrix} -g_j & 1 \\ -g_j & -1 \end{pmatrix}. \tag{4.8}$$

If we write (Z_j') for the value of (Z) at one film surface $z = z_j$, and (Z_j) for the value at $z = z_j + \delta_j$, we have the relation

$$(Z_j') = (P_j)(Z_j), \tag{4.9}$$

where

$$(P_j) = \begin{pmatrix} e^{i\psi_j} & 0 \\ 0 & e^{-i\psi_j} \end{pmatrix}, \psi_j \equiv p_j\delta_j. \tag{4.10}$$

Moreover, the boundary condition requiring continuity of the tangential field components at the interface of, say, the jth and $(j-1)$th films leads immediately to the continuity of (A), so that

$$(A_{j-1}) = (A_j'), \tag{4.11}$$

where the notation is analogous to that just described in (Z).

Combining (4.7), (4.9), and (4.11), we obtain the following recurrence relations for (Z_j):

$$\begin{aligned}(Z_{j-1}) = (T_{j-1})(A_{j-1}) &= (T_{j-1})(A_j') \\ &= (T_{j-1})(T_j)^{-1}(Z_j') \\ &= (T_{j-1})(T_j)^{-1}(P_j)(Z_j)\end{aligned} \tag{4.12}$$

and hence for (A_j),

$$\begin{aligned}(A_{j-1}) = (T_{j-1})^{-1}(Z_{j-1}) &= (T_j^{-1})(P_j)(T_j)(A_j) \\ &= (S_j)(A_j),\end{aligned} \tag{4.13}$$

where

$$(S_j) \equiv (T_j)^{-1}(P_j)(T_j). \tag{4.14}$$

This last expression is readily evaluated as

$$(S_j)_{\mathrm{TE}} = \begin{pmatrix} \cos\psi_j & (-i/g_j)\sin\psi_j \\ -ig_j\sin\psi_j & \cos\psi_j \end{pmatrix}, \tag{4.15}$$

which is identical with the corresponding Abelès[90] matrix (M_j).

If we now apply the recurrence relation (4.13) repeatedly over the entire set of L films, we relate the vacuum (A_0) to the bulk value (A_{L+1}) by

$$(A_0) = (Q)(A_{L+1}), \tag{4.16}$$

where

$$(Q) \equiv \prod_{j=1}^{L} (S_j). \tag{4.17}$$

Then if q_{mn} are the matrix elements of (Q), we have the following relationships between the incident, reflected, and transmitted electric vectors E_{yi}, E_{yr}, and E_{yt}:

$$\begin{aligned}E_{yi} + E_{yr} &= (q_{11} - g_b q_{12})E_{yt} \\ -\cos\varphi(E_{yi} - E_{yr}) &= (q_{21} - g_b q_{22})E_{yt}.\end{aligned} \tag{4.18}$$

In (4.18), g_b is simply the bulk (here Drude) value of g. We immediately obtain the complex amplitude reflection coefficients in the form

$$r_s \equiv \frac{E_{yr}}{E_{yi}} = \frac{\cos\varphi\,(q_{11} - g_b q_{12}) - (g_b q_{22} - q_{21})}{\cos\varphi\,(q_{11} - g_b q_{12}) + (g_b q_{22} - q_{21})}. \tag{4.19}$$

In the limit of a sharp surface the ψ_j vanish and r_s becomes the familiar expression

$$\begin{aligned}r_s(\text{sharp surface}) &= \frac{\cos\varphi - g_b}{\cos\varphi + g_b} \\ &= \frac{\cos\varphi - (\epsilon_b - \sin^2\varphi)^{1/2}}{\cos\varphi + (\epsilon_b - \sin^2\varphi)^{1/2}}.\end{aligned} \tag{4.20}$$

In the case of the TM wave the (S_j) are found to be

$$(S_j)_{\mathrm{TM}} = \begin{pmatrix} \cos\psi_j & (i/h_j)\sin\psi_j \\ ih_j\sin\psi_j & \cos\psi_j \end{pmatrix}. \tag{4.21}$$

If the elements of (Q) are Q_{mn}, use of (4.21) leads to an amplitude reflection coefficient given by

$$r_p = \frac{(Q_{11} + h_b Q_{12}) - \cos\varphi\,(Q_{21} + h_b Q_{22})}{(Q_{11} + h_b Q_{12}) + \cos\varphi\,(Q_{21} + h_b Q_{22})}. \tag{4.22}$$

Again, as the ψ_j approach zero (4.22) reduces to the usual form

$$r_p(\text{sharp surface})=\frac{(\epsilon_b-\sin^2\varphi)^{1/2}-\epsilon_b\cos\varphi}{(\epsilon_b-\sin^2\varphi)^{1/2}+\epsilon_b\cos\varphi}. \quad (4.23)$$

The energy reflection coefficients ($R_s=r_sr_s^*$, $R_p=r_pr_p^*$) and the ellipsometric properties are obtained from (4.19) and (4.22) in the conventional manner. The important feature of this treatment, however, is that a given set of these properties is not unique to a single set of films. Herpin demonstrates that any product of two or more (S_j) can be expressed as a sum of Pauli matrices, and hence that the optical properties of an arbitrary stratified medium are equivalent to those of a system of two appropriately chosen homogeneous films. The proof of this theorem leads directly to the conclusion that there are possible an infinite number of such media which are optically equivalent to any given double layer.

The consequences for our calculation are far reaching. They assert that in choosing and parametrizing a particular conductivity profile for our surface zone, we are in effect choosing an equivalent double layer. Since there are an infinite number of possible profiles equivalent to the same double layer, it follows that the conclusions we shall reach from our calculation are independent of the particular form we have chosen. Admittedly, this implies that we have no direct way of confirming the physical speculations that led us to our choice of profile; on the other hand, it encourages us not to be unduly upset if parameters that are physically unlikely are required to fit our choice of profile to the observed data.

With these qualifications in mind we return to the calculation itself. We choose a value for the effective width, 2Δ, of the Epstein profile, and extend our stratified medium over a range $\pm 10\Delta$ about the plane $z=0$, assuming that the medium has the properties of the vacuum for $z<-10\Delta$ and of homogeneous bulk mercury for $z>+10\Delta$. We divide the intermediate range into 100 thin homogeneous films of equal width, and determine the complex dielectric constant, ϵ_j, of the film by evaluating the Epstein profile at $z=z_j$. We have tested the adequacy of this approximation by extending the range to $\pm 15\Delta$, and also by increasing the number of films in the $\pm 10\Delta$ range to 200. We find that our results are not materially affected.

Throughout most of the range cited, we assign to the surface conductivity parameter σ_s the free-electron form $\sigma_s=\sigma_{0s}/(1+i\omega\tau_s)$, where the surface dc conductivity σ_{0s} and the surface relaxation time τ_s are treated as separately variable parameters.

The contribution from $\sigma_s(\omega)$ rises from zero in the bulk to a maximum value of $\frac{1}{4}\sigma_s(\omega)$ at $z=0$, then drops as we approach the vacuum. If this drop reflects the drop in density from our density maximum, we should expect localized states to appear before the $\sigma_s(\omega)$ contribution reaches zero. Mott estimates that this will occur for a 12% linear expansion, or a decrease of about 30% in the density. This estimate may be inaccurate for a close-packed liquid, but we nevertheless adopt it and change the form of $\sigma_s(\omega)$ abruptly to a Lorentzian when its coefficient $-w/(1-w)^2$ has dropped to 70% of its maximum value. We center the Lorentzian about the approximate location of the maximum in Hodgson's $\omega\epsilon_2(\omega)$, $\hbar\omega_0=0.6$ eV. We find, however, that our results can be fitted to the data equally well using Mott's[12] estimate $\hbar\omega_0\sim 1.1$ eV. For simplicity we let the height of our Lorentzian be given by σ_{0s} and its half-width by $1/\tau_s$.

With our profile so defined we can compute the amplitude reflection coefficients r_s and r_p from formulas (3.19) and (4.22) for each value of 2Δ over a mesh of values of σ_{0s} and τ_s. We are interested in three angles of incidence: $\varphi=0$ (normal incidence), corresponding to our own experiments and those of Boiani and Rice[38] and Wilson and Rice[32]; $\varphi=45°$, corresponding to the work of Schulz;[28] and $\varphi=78.05°$, corresponding to the work of Faber and Smith,[34] and, to a close approximation, to that of Hodgson[30] (who used $\varphi\sim 80°$). At each angle we calculate from r_s and r_p the apparent optical quantities ϵ_1 and $\omega\epsilon_2$ as obtained from the sharp-surface ellipsometric formulas used by Hodgson and by Faber and Smith, and also the quantity $\bar{R}=\frac{1}{2}(R_s+R_p)$ measured by Schulz. At $\varphi=0$, this last is, of course, just the reflectivity at normal incidence, R_N. Finally, we repeat the procedure for each of the 17 wavelengths at which measurements were made by either Faber and Smith or Hodgson.

We seek values of 2Δ, $\frac{1}{4}\sigma_{0s}$, and τ_s which would have led to ellipsometric values of ϵ_1 and $\omega\epsilon_2$ close to those of Faber and Smith and of Hodgson, but also to the $\bar{R}$ of Schulz and to our own R_N. As 2Δ is increased, we find, quite expectedly, that such results are obtained at lower and lower values of $\frac{1}{4}\sigma_{0s}$ (although it is always larger than σ_{0b}, the experimental bulk dc conductivity), but that the appropriate value of τ_s stays within 10% or so of the classical bulk relaxation time τ_b. The best fit (in a rather coarse mesh) was obtained using the improbable values $2\Delta=2$ Å, $\frac{1}{4}\sigma_{0s}=12\sigma_{0b}$, and $\tau_s=0.9\tau_b$. At the expense of an additional disagreement of about 0.5% in the reflectivities, an otherwise comparable fit can be obtained with more reasonable parameters, such as, for example, $2\Delta=10$ Å, $\frac{1}{4}\sigma_{0s}=2.5\sigma_{0b}$, and $\tau_s=1.0\tau_b$.

To confirm the legitimacy of this result we have obtained a similar and even somewhat closer fit using a substantially different profile. We skew the Epstein form by choosing different values Δ_1 and Δ_2 of Δ on the vapor and bulk sides of the maximum, respectively. The effective profile width is now $\Delta_1+\Delta_2$. If we characterize the films on the bulk side by the free-electron form, and those on the vapor side by a Lorentzian centered about 0.8 eV, we obtain good agreement at $\Delta_1=1$ Å, $\Delta_2=5$ Å, $\frac{1}{4}\sigma_{0s}=4.25\sigma_{0b}$, $\tau_s=0.9\tau_b$. This profile is virtually equivalent to the same double layer as our original one, and

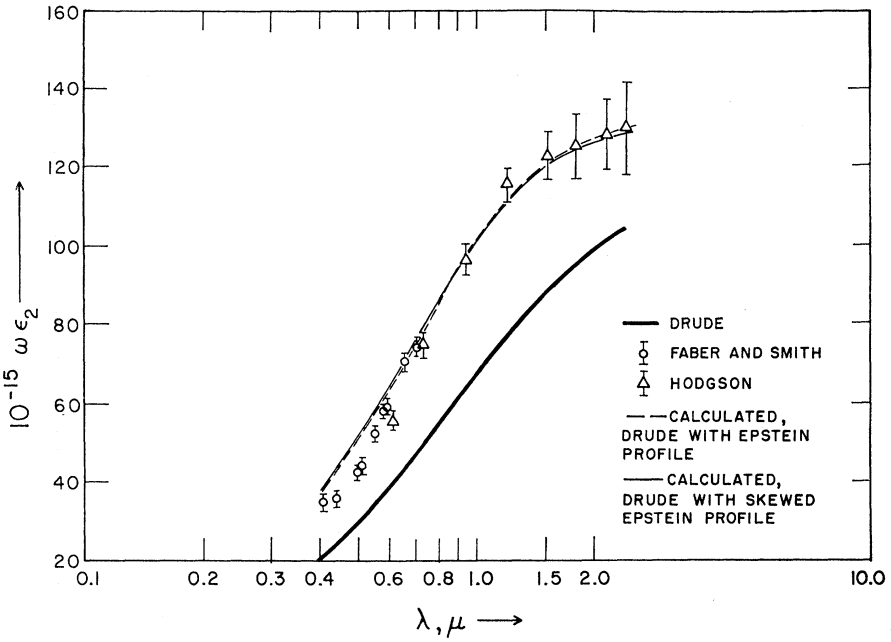

FIG. 9. Effect of a surface transition zone on ellipsometrically determined $\omega\epsilon_2$ for mercury, $\varphi=78.05°$. The theoretical curves in this and the next three figures were calculated using parameters chosen to give the best simultaneous fit to the data of Hodgson (Ref. 30) and Faber and Smith (Ref. 34) (this figure and Fig. 10), of Schulz (Ref. 28) (Fig. 11), and of this work (Fig. 12). The sharp-surface Drude curve is given in each figure for comparison.

there is no reason not to expect that further modification would produce very similar results with still more realistic parameters. But in view of the theorem of Herpin discussed above, we are inclined to accept the best fit and to view the credibility of our parameters as a measure of the appropriateness of our choice of profile, and not of the validity of our basic hypothesis that a surface effect does appear.

Figure 9, then, is a plot against wavelength of $\omega\epsilon_2(\omega)$ as it would appear in an ellipsometric measurement of liquid mercury at $\varphi=78.05°$ in the presence of our Epstein conductivity profile with $2\Delta=2$ Å, $\frac{1}{4}\sigma_{0s}=12\sigma_{0b}$, and $\tau_s=0.9\tau_b$, and of our modified profile with $\Delta_1=1$ Å, $\Delta_2=5$ Å, $\frac{1}{4}\sigma_{0s}=4.25\sigma_{0b}$, and $\tau_s=0.9\tau_b$. The lines representing our calculations are to be compared with the experimental points of Faber and Smith and of Hodgson. For reference, the Drude curve is also plotted. Figure 10 is a similar plot of ϵ_1. The agreement between calculation and experiment in both parts of the dielectric constant speaks for itself.

Figure 11 plots $\bar{R}$ at $\varphi=45°$ for the same profiles. The close agreement with the Drude curve, and hence with

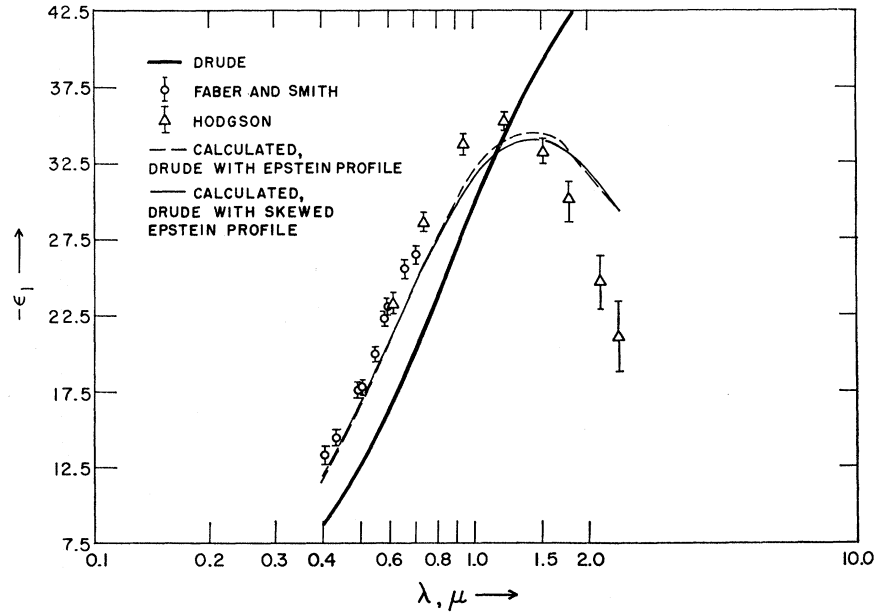

FIG. 10. Effect of a surface transition zone on ellipsometrically determined ϵ_1 for mercury, $\varphi=78.05°$. Calculations as in Fig. 9.

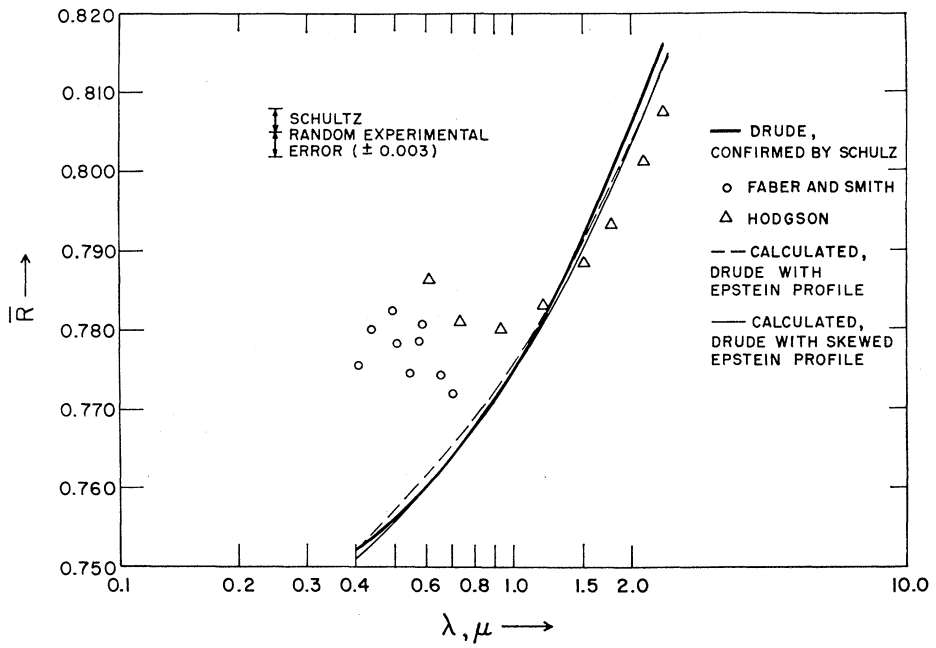

FIG. 11. Effect of a surface transition zone on $\bar{R}=\frac{1}{2}(R_s+R_p)$ for a mercury-vacuum interface at $\varphi=45°$, corresponding to the work of Schulz (Ref. 28). Calculations as in Fig. 9. The data of Faber and Smith (Ref. 34) and of Hodgson (Ref. 30) have been recalculated to 45° incidence, assuming a sharp surface, for comparison.

Schulz, is to be contrasted with the locations of the points representing the results that should have appeared if Faber-Smith-Hodgson mercury having a sharp surface were measured in this way. The result at normal incidence (Fig. 12) is not quite so impressive, but still shows markedly the contrast between our calculation and the ellipsometric data recalculated to give the reflectivity at normal incidence. It is to be noted that our results differ appreciably from the Drude curve only in a wavelength region where the precision of most of the experiments performed to date is poor enough to hide the deviation. The difference between the ellipsometric and absolute reflectivity results, on the other hand, is outside the experimental uncertainty of any of the studies cited.

It seems safe to assert, in conclusion, that there does exist some physically reasonable conductivity profile which accounts for all of the optical data in liquid mercury. Whether this is also true of all other liquid metals with structure-sensitive low conductivity re-

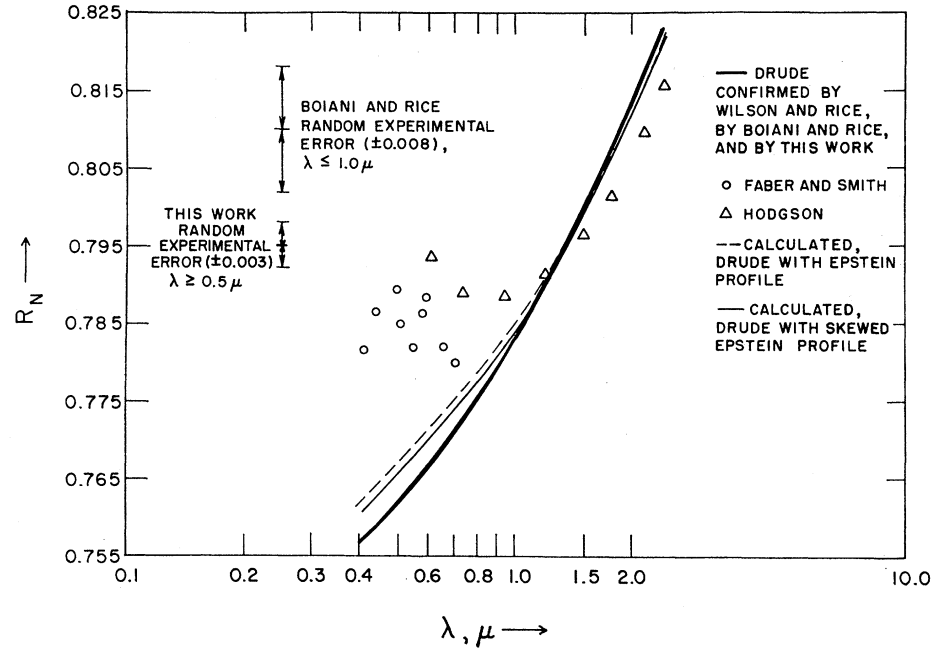

FIG. 12. Effect of a surface transition zone on reflectivity at normal incidence R_N of a mercury-vacuum interface. Calculations as in Fig. 9; recalculation of ellipsometric data to normal incidence as in Fig. 11. The magnitude of the effect can be judged from the experimental errors indicated.

mains to be established, since most of the reliable measurements on these metals so far have been ellipsometric. Where absolute reflectivities have been determined, however, discrepancies have usually been found. For example, while both Hodgson[30] and Schulz[92] are able to fit the Drude curve for liquid indium, Hodgson can do so only with an "effective number of electrons" larger than the number of valence electrons. Meanwhile, Wilson and Rice,[32] operating at normal incidence, obtain reflectivities substantially below the Drude values. A similar disagreement between Hodgson[93] and Wilson and Rice[32] arises in the case of molten bismuth.

Clearly, more absolute reflectivity determinations are in order, not only on liquid metals but also on transitional systems such as the metal-molten salt systems. In particular, the results of our calculations indicate that measurements of the dependence of the absolute reflection coefficients R_s and R_p (as opposed to ellipsometric measurements) on angle of incidence at oblique angles would cast considerable light on the nature of the surface zone. To amplify this point, in Table I we display the variation with angle of incidence of calculated apparent ellipsometric optical constants for liquid Hg at a wavelength of 5461 Å. To well within the $\pm 2\%$ precision quoted by Faber and Smith, these values are constant over the range of angles of incidence for which ellipsometric measurements are possible.

Studies of the temperature and pressure dependence of optical surface effects would also be invaluable. It is hoped that the concepts and the instrument described in this paper will be helpful to such studies, as well as to the investigation of surface phenomena in general.

TABLE I. Expected variation of ϵ_1 and ϵ_2 as a function of angle of incidence of the light for a liquid metal with a surface variation of the conductivity.

φ (deg)	$-\epsilon_1$	$\omega\epsilon_2$ (10^{16} cps)
50	18.76	5.825
55	18.77	5.827
60	18.79	5.829
65	18.80	5.831
70	18.81	5.832
75	18.82	5.834
80	18.82	5.834
85	18.83	5.835

ACKNOWLEDGMENTS

The authors are grateful to Dr. David Beaglehole, whose helpful and original suggestions contributed substantially to the early phases of construction of the apparatus. We wish to thank the Directorate of Chemical Sciences, Air Force Office of Scientific Research, for financial support. We have also benefitted from the use of facilities provided by the Advanced Research Projects Agency for materials research at the University of Chicago. A.N.B. would like to thank the National Science Foundation and the Shell Foundation for fellowships in 1964–66 and 1966–67, respectively.

[92] L. G. Schulz, J. Opt. Soc. Am. 47, 70 (1956).
[93] J. N. Hodgson, Phil. Mag. 7, 229 (1962).